

DIG-MILP: a Deep Instance Generator for Mixed-Integer Linear Programming with Feasibility Guarantee

Haoyu Wang

Georgia Tech

haoyu.wang@gatech.edu

Jialin Liu

Damo Academy, Alibaba US

jialin.liu@alibaba-inc.com

Xiaohan Chen

Damo Academy, Alibaba US

xiaohan.chen@alibaba-inc.com

Xinshang Wang

Damo Academy, Alibaba US

xinshang.w@alibaba-inc.com

Pan Li

Georgia Tech

panli@gatech.edu

Wotao Yin

Damo Academy, Alibaba US

wotao.yin@alibaba-inc.com

Reviewed on OpenReview: <https://openreview.net/forum?id=MywlrEaFqR>

Abstract

Mixed-integer linear programming (MILP) stands as a notable NP-hard problem pivotal to numerous crucial industrial applications. The development of effective algorithms, the tuning of solvers, and the training of machine learning models for MILP resolution all hinge on access to extensive, diverse, and representative data. Yet compared to the abundant naturally occurring data in image and text realms, MILP is markedly data deficient, underscoring the vital role of synthetic MILP generation. We present DIG-MILP, a deep generative framework adept at extracting deep-level structural features from highly limited MILP data and producing instances that closely mirror the target data. Notably, by leveraging the MILP duality, DIG-MILP guarantees a correct and complete generation space as well as ensures the boundedness and feasibility of the generated instances. Our empirical study highlights the novelty and quality of the instances generated by DIG-MILP through two distinct downstream tasks: (S1) We identify Data Sharing, which involves MILP solver tuning without directly sharing the original data. Experiments show that solver solution time on instances generated by Dig-MILP correlate highly positively with the original data, offering a potential solution direction.; (S2) Data Augmentation, wherein the DIG-MILP-generated instances bolster the generalization performance of machine learning models tasked with resolving MILP problems.

1 Introduction

Mixed integer linear programming (MILP) is a prominent problem central to operations research (OR) (Achterberg & Wunderling, 2013; Wolsey, 2020). It forms the basis for modeling numerous crucial industrial applications, including but not limited to supply chain management (Hugos, 2018), production scheduling (Branke et al., 2015), financial portfolio optimization (Mansini et al., 2015), and network design (Al-Falahy & Alani, 2017; Radosavovic et al., 2020). This article aims to answer the question: *How can one produce a series of high-quality MILP instances?* The motivation behind this inquiry is illustrated

through the subsequent scenarios, where the definition of "high-quality" varies based on the specific requirements of each context.

(Scenario I). In industry, clients from real-world business seek specialized companies to develop or fine-tune intricate solver systems (Cplex, 2009; Bestuzheva et al., 2021; Gurobi, 2023) for solving MILP problems. The empirical success of the systems heavily depends on well-tuned hyper-parameters for the solvers, which demands ample and representative testing cases that accurately reflect the actual cases. However, real data is often scarce during the early stages of a business. In addition, clients are typically reluctant to publish data that might encompass some specific information (e.g., schedules or contract stipulations for flight arrangement (Richards & How, 2002; Roling et al., 2008), platform costs or audience data for ad placements (Rodríguez et al., 2016)). In this scenario, the goal is to generate new instances randomly, without sensitive information, but with similar solution times across different settings. By sharing these synthetic instances with solver developers, they can refine algorithms or configurations based on these instances, thereby gaining valuable insights and potentially applying these improvements directly to real-world cases.

(Scenario II). Beyond the development and testing of MILP algorithms by domain experts (Lawler & Wood, 1966; Gamrath et al., 2015), recent efforts have explored machine learning (ML) to derive heuristic algorithms directly from data (Khalil et al., 2016; 2017; Nair et al., 2020). The effectiveness of ML-driven methods heavily relies on the availability of extensive and representative training data (Lu et al., 2022). Given the scarcity of MILP instances compared to other data types like images or texts, there arises a necessity for instance generation. In this scenario, the objective is to augment the training data to improve the generalization performance of ML models on MILP tasks.

Both scenarios underscore the motivation to synthetically generate novel instances that resemble the limited existing MILP data. Compared with some existing methods tailored to specific problems (e.g., knapsack (Hill et al., 2011) and quadratic assignment (Drugan, 2013)), our approach focuses on a more **general framework** for MILP generation. We aim for our proposed method to be capable of generating instances for a variety of problems, as long as they can be formulated as MILPs. This general-purpose MILP generator potentially has wider applications compared to more specialized solutions.

A major challenge in synthetic MILP generation is ensuring **representativeness**. This demands that the generated instances should closely mirror the original data in terms of scale, modeling logic (the structure of the objective and constraints), and key mathematical properties such as feasibility and boundedness.

In this paper, we are particularly interested in generating **feasible and bounded** MILP instances. In many applications, practitioners are required to formulate feasible and bounded MILPs; otherwise, adjustments to the formulas or numerical values are necessary. Take, for instance, the Unit Commitment problem in power grid systems. The goal is to determine which power generation units should be turned on or off to meet energy demands at the lowest cost, adhering to operational constraints like minimum downtime and startup times. The problem must be feasible to ensure there is always enough generation capacity online to meet demand. An infeasible solution means that there is no possible combination of on/off statuses for generation units that meet the required demand. Unfortunately, a randomly generated MILP with naive approaches is likely to be infeasible or unbounded.¹ Given that determining the feasibility of an MILP is NP-Complete (Conforti et al., 2014; Hartmanis, 1982), methods that simply generate and then discard infeasible instances are inefficient. Thus, there is a clear need for generating MILPs with guaranteed feasibility and boundedness.

Existing methods for MILP generation fall short of fulfilling the criteria above. Some approaches generate new instances in an embedding space with handcraft statistics (Smith-Miles & Bowly, 2015; Bowly, 2019). These methods model MILPs' coefficients with simple distributions such as Gaussian, generating instances with very limited structural characters that may not be representative enough. A concurrent paper (Geng et al., 2024) with our work learn the MILP distribution over instance space with neural networks (NNs). The generated instances from Geng et al. (2024) do not enjoy feasibility-boundedness guarantee. By employing deep neural networks (NNs) to extract the in-depth structural information, our proposed method DIG-MILP generates "representative" data that resembles the original samples without expert knowledge.

¹As noted in Section 4.1 of (Bowly et al., 2020), only 37.5% of the LP instances generated by naive methods are feasible and bounded, and this proportion decreases further when integer constraints are involved.

Additionally, DIG-MILP leverages the MILP duality theories to ensure the feasibility and boundedness of each generated instance by controlling its primal format and the dual format of its linear relaxation having at least a feasible solution, which achieves the “feasibility-boundedness” of the generated data. Moreover, any feasible-bounded MILP is inside the generation space of DIG-MILP, meeting the demand for “generality”. An illustration of DIG-MILP’s generation strategy is shown in Figure. 1. Recognizing the limited original data along with the requirements on scalability and numerical precision in MILP generation, instead of generating from scratch, DIG-MILP iteratively modifies parts of existing MILPs, allowing control on the degree of structural similarity towards the original data.

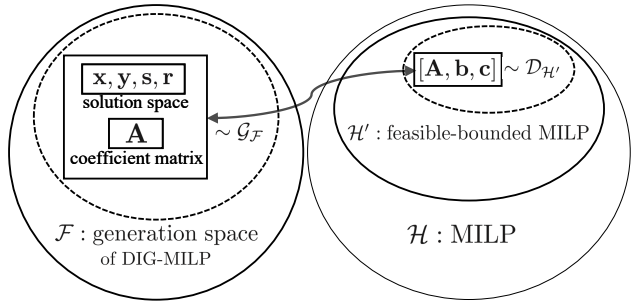


Figure 1: DIG-MILP generates feasible-bounded instances that resemble the target MILP data from distribution $\mathcal{D}_{\mathcal{H}'}$ by learning to sample the coefficient matrix along with a set of feasible solutions for both the primal format and dual format of the linear relaxation from the corresponding distribution $\mathcal{G}_{\mathcal{F}}$. See detailed explanations in Section. 3.

We conduct two downstream tasks to validate the quality and novelty of DIG-MILP-generated instances, corresponding to the motivation of data generation in industry and in academia respectively. The first task is to measure whether the examples generated by DIG-MILP show a positive correlation in terms of the time required to solve them on the solver with the same hyper-parameters, compared to the original examples.

Across four problems, the solution time of solver SCIP (Bestuzheva et al., 2021) exhibits a highly positive correlation between the DIG-MILP-generated instances and the original data w.r.t. different hyper-parameter sets. The experiments can be viewed as a preliminary attempt to address the issue from **(scenario I)** using deep generative models and provide a potentially promising research direction. To completely solve the problem would require further research effort. The other task is envisioned as data augmentation, where the generated instances are used to enhance the performance of an important proxy task for exploring how neural networks (NN) solve MILP problems. Specifically, it helps assist in training NNs to predict the optimal objective values for MILP problems (Chen et al., 2023). Models trained on datasets augmented with DIG-MILP-generated instances demonstrate enhanced generalization capabilities.

2 Related Work

In the following, we discuss works on MILP generation and works on generative models.

In light of Hooker’s proposals (Hooker, 1994; 1995), research on MILP generation diverges into two paths. The first focuses on leveraging expert domain knowledge to create generators for specific problems such as set covering (Balas & Ho, 1980), traveling sales person (Pilcher & Rardin, 1992; Vander Wiel & Sahinidis, 1995), graph colouring (Culberson, 2002), knapsack (Hill et al., 2011), and quadratic assignment (Drugan, 2013). This specificity causes poor generalization across different problems and thus fails to meet the generality criterion. In contrast, the second path aims at generating general MILPs. Asahiro et al. (1996) propose to generate completely random instances, which is inadequate for producing instances with specific distributional features (Hill & Reilly, 2000). Bowly (2019); Bowly et al. (2020) attempt to sample feasible instances similar to target data by manually controlling distributions in an embedding space. Its manual feature extraction and statistic control by simple distributions leads to instances with limited structural characteristics. A concurrent work Geng et al. (2024) adopts NNs to further improve the expressive capability of the instance generator in Bowly (2019) and thus achieves more similar instances, yet the framework does not produce instances with boundedness-feasibility guarantees. Inspired by Bowly (2019), DIG-MILP generates instances from the solution space and uses DNNs to dig out more details, aiming to delineate the structural attributes more precisely and generate feasible-bounded instances.

Recent years have witnessed the fast development of generative models, such as GAN Creswell et al. (2018), VAE Kipf & Welling (2016), and diffusion models Ho et al. (2020); Song & Ermon (2019). Considering the training complexity, and the strongly-structured MILP instances, we adopt VAE as the generative backbone

in this paper, and we leave the utilization of more advanced generative models with potentially higher training computational cost as a feature direction to explore.

3 Methodology

We start by providing a preliminary background on MILP generation. Subsequently, we discuss the theoretical foundation based on which DIG-MILP’s generation strategy ensures the feasibility and boundedness of its generated instances. Finally, we delve into the training and inference process of DIG-MILP along with its neural network architecture.

3.1 Preliminaries

Given a triplet of coefficient matrix $\mathbf{A} \in \mathbb{R}^{m \times n}$, right-hand side constant $\mathbf{b} \in \mathbb{R}^m$, and objective coefficient $\mathbf{c} \in \mathbb{R}^n$, an MILP is defined as:

$$\text{MILP}(\mathbf{A}, \mathbf{b}, \mathbf{c}) : \max_{\mathbf{x}} \mathbf{c}^\top \mathbf{x}, \quad \text{s.t. } \mathbf{A} \mathbf{x} \leq \mathbf{b}, \mathbf{x} \in \mathbb{Z}_{\geq 0}^n. \quad (1)$$

To solve MILP is to identify a set of non-negative integer variables that maximize the objective function while satisfying a series of linear constraints, which is NP-hard (Bulut & Ralphs, 2021). Within the entire MILP space $\mathcal{H} = \{[\mathbf{A}, \mathbf{b}, \mathbf{c}] : \mathbf{A} \in \mathbb{R}^{m \times n}, \mathbf{b} \in \mathbb{R}^m, \mathbf{c} \in \mathbb{R}^n\}$, many of MILP problems are infeasible (no \mathbf{x} satisfies all the constraints in (1)) or unbounded (the value of $\mathbf{c}^\top \mathbf{x}$ can grow indefinitely while still satisfying all the constraints). However, *In real-world scenarios, MILPs derived from practical issues are often either naturally or modified to be feasible, bounded, and yield an optimal solution*², as discussed in Section 1. Therefore, we are particularly interested in generating feasible-bounded MILPs from the space \mathcal{H}' as follows:³

$$\mathcal{H}' := \{[\mathbf{A}, \mathbf{b}, \mathbf{c}] : \mathbf{A} \in \mathbb{Q}^{m \times n}, \mathbf{b} \in \mathbb{Q}^m, \mathbf{c} \in \mathbb{Q}^n \text{ and MILP}(\mathbf{A}, \mathbf{b}, \mathbf{c}) \text{ is feasible and bounded.}\}.$$

It’s important to note that merely telling the feasibility of such a problem is NP-Complete (Conforti et al., 2014; Hartmanis, 1982), and its special case (the binary case) is listed in one of the Karp’s 21 problems (Karp, 2010). Thus, the task of reliably generating MILPs from \mathcal{H}' is far from trivial.

Suppose a target MILP dataset D that models a particular business scenario is sampled from a distribution $\mathcal{D}_{\mathcal{H}'}(\mathbf{A}, \mathbf{b}, \mathbf{c})$ defined on \mathcal{H}' , the task of MILP instance generation is to approximate the distribution $\mathcal{D}_{\mathcal{H}'}$ and sample novel MILP instances from it.

3.2 DIG-MILP with Feasibility Guarantee

An intuitive idea for MILP generation is to directly sample $[\mathbf{A}, \mathbf{b}, \mathbf{c}]$ from $\mathcal{D}_{\mathcal{H}'}$, which is practically hard to implement as it’s hard to guarantee the generated instance to be feasible-bounded.

According to MILP duality theories, we observe that as long as DIG-MILP ensure that a generated instance’s primal format $\text{MILP}(\mathbf{A}, \mathbf{b}, \mathbf{c})$ and the dual format of its linear relaxation $\text{DualLP}(\mathbf{A}, \mathbf{b}, \mathbf{c})$ (as defined in Equation. 2) both have at least one set of feasible solutions, then the newly generated instance will be guaranteed to be feasible-bounded (as proved in Proposition. 1).

$$\text{DualLP}(\mathbf{A}, \mathbf{b}, \mathbf{c}) : \min_{\mathbf{y}} \mathbf{b}^\top \mathbf{y}, \quad \text{s.t. } \mathbf{A}^\top \mathbf{y} \geq \mathbf{c}, \mathbf{y} \geq 0, \quad (2)$$

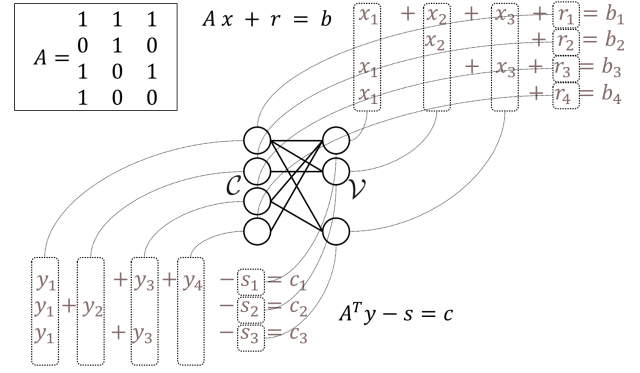
To guarantee the existence of feasible solutions to both problems, inspired by (Bowly, 2019), we propose to sample the instances from another space \mathcal{F} , where

$$\mathcal{F} := \{[\mathbf{A}, \mathbf{x}, \mathbf{y}, \mathbf{s}, \mathbf{r}] : \mathbf{A} \in \mathbb{Q}^{m \times n}, \mathbf{x} \in \mathbb{Z}_{\geq 0}^n, \mathbf{y} \in \mathbb{Q}_{\geq 0}^m, \mathbf{s} \in \mathbb{Q}_{\geq 0}^n, \mathbf{r} \in \mathbb{Q}_{\geq 0}^m\}. \quad (3)$$

²Definitions of boundedness, feasibility, and optimal solution of MILP in Definition. 1 2 3 in the appendix.

³Narrowing from the real domain to the rational domain is common in MILP studies to avoid cases where an MILP is feasible and bounded but lacks an optimal solution Schrijver (1998). For example, $\min \sqrt{3}x_1 - x_2, \text{ s.t. } \sqrt{3}x_1 - x_2 \geq 0, x_1 \geq 1, \mathbf{x} \in \mathbb{Z}_{\geq 0}^2$. No feasible solution has objective equal to zero, but there are feasible solutions with objective arbitrarily close to zero.

object	feature
constraint nodes: $\mathcal{C} = \{c_1 \dots c_m\}$	$\mathbf{y} = [y_1, \dots, y_m]^\top$ $\mathbf{r} = [r_1, \dots, r_m]^\top$
variable nodes: $\mathcal{V} = \{v_1 \dots v_n\}$	$\mathbf{x} = [x_1, \dots, x_n]^\top$ $\mathbf{s} = [s_1, \dots, s_n]^\top$
edge \mathcal{E}	non-zero weights in \mathbf{A}

 Table 1: Nodes and edges' attributes in G .

 Figure 2: An example of bipartite graph representation with 4 nodes in set \mathcal{C} and 3 nodes in set \mathcal{V} .

\mathcal{F} defines an alternative space to represent feasible-bounded MILPs, with each element $[\mathbf{A}, \mathbf{x}, \mathbf{y}, \mathbf{s}, \mathbf{r}]$ consisting of the coefficient matrix \mathbf{A} along with a set of feasible solutions \mathbf{x}, \mathbf{y} to $\text{MILP}(\mathbf{A}, \mathbf{b}, \mathbf{c})$ and $\text{DualLP}(\mathbf{A}, \mathbf{b}, \mathbf{c})$, respectively, where \mathbf{b}, \mathbf{c} are determined by the corresponding slacks \mathbf{s}, \mathbf{r} via the equalities defined in Equation. 4. By leveraging this idea, DIG-MILP aims to learn a distribution $\mathcal{G}_{\mathcal{F}}$ over the space of \mathcal{F} to sample $[\mathbf{A}, \mathbf{x}, \mathbf{y}, \mathbf{s}, \mathbf{r}]$, which can be further transformed into $[\mathbf{A}, \mathbf{b}, \mathbf{c}]$ that defines an MILP problem based on Equation. 4.

$$\text{Slack Variables: } \mathbf{Ax} + \mathbf{r} = \mathbf{b}, \mathbf{A}^\top \mathbf{y} - \mathbf{s} = \mathbf{c}, \quad \text{where } \mathbf{r} \in \mathbb{Q}_{\geq 0}^m, \mathbf{s} \in \mathbb{Q}_{\geq 0}^n \quad (4)$$

Such a generation strategy offers theoretical guarantees on the boundedness and feasibility of the generated instances, ensuring the “feasibility-boundedness” of the produced data. Moreover, all the feasible and bounded MILPs in \mathcal{H}' correspond to at least a tuple $[\mathbf{A}, \mathbf{x}, \mathbf{y}, \mathbf{s}, \mathbf{r}]$. In other words, generating tuples in the form of $[\mathbf{A}, \mathbf{x}, \mathbf{y}, \mathbf{s}, \mathbf{r}]$ instead of generating $[\mathbf{A}, \mathbf{b}, \mathbf{c}]$ directly is a general approach for producing feasible and bounded instances. This is formally stated in Proposition. 1. See detailed proof in A.1 in the appendix.

Proposition 1 (Boundedness and Feasibility Guarantee of DIG-MILP). Denote \mathcal{H}'' as the DIG-MILP-generating space:

$$\mathcal{H}'' := \left\{ [\mathbf{A}, \mathbf{b}, \mathbf{c}] : \mathbf{b} = \mathbf{Ax} + \mathbf{r}, \mathbf{c} = \mathbf{A}^\top \mathbf{y} - \mathbf{s}, [\mathbf{A}, \mathbf{x}, \mathbf{y}, \mathbf{s}, \mathbf{r}] \in \mathcal{F} \right\}.$$

It holds that this generating space is exactly equal to \mathcal{H}' : $\mathcal{H}'' = \mathcal{H}'$.

3.3 Generation Process and Architecture

Having shown the equivalence between spaces \mathcal{F} and \mathcal{H}' , we then present how DIG-MILP learns a distribution $\mathcal{G}_{\mathcal{F}}$ to sample $[\mathbf{A}, \mathbf{x}, \mathbf{y}, \mathbf{s}, \mathbf{r}]$ from. The key concept is as follows: We first conceptualize $[\mathbf{A}, \mathbf{x}, \mathbf{y}, \mathbf{s}, \mathbf{r}]$ as a bipartite graph, thus transforming the generation of these elements into a *graph generation* problem. To train a model capable of generating such graphs, we employ an autoregressive method: iteratively removing a node from the graph, and then using a neural network to predict and restore the removed node’s edges and attributes. During inference, we randomly select and remove a node from the current graph, and then use the trained neural network to reconstruct it. This process is repeated to generate a new graph.

Graph Representation. Here, we detail the representation of $[\mathbf{A}, \mathbf{x}, \mathbf{y}, \mathbf{s}, \mathbf{r}]$ as a bipartite graph within a variable-constraint (VC) framework, denoted as graph $G(\mathcal{V}, \mathcal{C}, \mathcal{E})$. Inspired by (Gasse et al., 2019), we treat each MILP variable as a node in \mathcal{V} , labeled v_j , where $j = 1, 2, \dots, n$. The j -th element in \mathbf{x} and \mathbf{s} , x_j and s_j , are attributes associated with node v_j . Similarly, each MILP constraint is represented as a node in \mathcal{C} , denoted by c_i , with $i = 1, 2, \dots, m$. The elements y_i and r_i are attributes linked to node c_i . An edge $e_{i,j}$ in \mathcal{E} connects a variable node v_j in \mathcal{V} to a constraint node c_i in \mathcal{C} if the coefficient $a_{i,j}$ in the matrix \mathbf{A} is non-zero, indicating that the j -th variable contributes to the i -th constraint of the system $\mathbf{Ax} \leq \mathbf{b}$ in MILP (1). Therefore, \mathbf{A} can be considered as the adjacency matrix of graph G . Figure 2 illustrates this graph

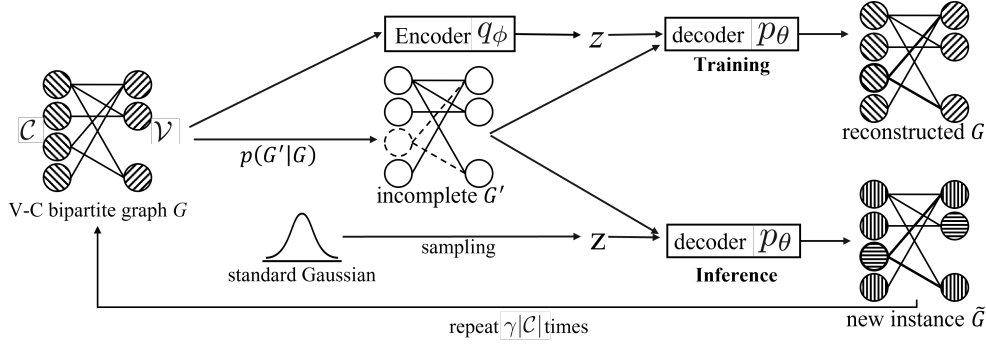


Figure 3: The training and inference pipeline of DIG-MILP. In each training step, DIG-MILP removes a random constraint node, its connected edges, along with the solution and slack features on all the nodes, resulting in an incomplete graph G' . The training objective of DIG-MILP is to reconstruct G from G' and \mathbf{z} sampled by the encoder q_ϕ . As to inference, DIG-MILP employs an auto-regressive approach, generating new instances by iteratively modifying the existing MILPs.

representation with a 4×3 example. The attributes of nodes and edges are detailed in Table. 1. With this graph representation, we transform the MILP generation problem into a graph generation task.

Generation pipeline. We display the training and inference pipeline in Figure. 3. As illustrated in Algorithm. 1, on each training step of DIG-MILP, we randomly select and remove a constraint node c_i (corresponding to the i -th constraint) from the bipartite graph, along with all its connected edges $\mathcal{E}_G(c_i)$. Concurrently, we erase the features of the solution space $\mathbf{x}, \mathbf{y}, \mathbf{s}, \mathbf{r}$ on all the nodes, resulting in an incomplete graph $G'(\mathcal{C} \setminus c_i, \mathcal{V}; \mathcal{V}_{-\mathbf{x}, \mathbf{r}}; \mathcal{E} \setminus \mathcal{E}_G(c_i))$. The training objective is to learn DIG-MILP to reconstruct G from the given G' by maximizing the log likelihood:

$$\arg \max_{\theta, \phi} \mathbb{E}_{G \sim D} \mathbb{E}_{G' \sim p(G'|G)} \log \mathbb{P}(G|G'; \theta, \phi), \quad (5)$$

where $p(G'|G)$ denotes the aforementioned process of randomly removing a node and its connected edges to obtain the incomplete graph. We adhere to standard VAEs (Kingma & Welling, 2013; Kipf & Welling, 2016) and introduce latent variable $\mathbf{z} = [z_1, \dots, z_{m+n}]$ with the assumption that \mathbf{z} is independent with G' . Utilizing ELBO, we endeavor to maximize the training objective through the optimization of the following loss function:

$$\min_{\theta, \phi} \mathcal{L}_{\theta, \phi} = \mathbb{E}_{G \sim D} \mathbb{E}_{G' \sim p(G'|G)} \left[\alpha \mathbb{E}_{\mathbf{z} \sim q_\phi(\mathbf{z}|G)} [-\log p_\theta(G|G', \mathbf{z})] + \mathcal{D}_{KL}[q_\phi(\mathbf{z}|G) \|\mathcal{N}(0, I)] \right], \quad (6)$$

where the decoder p adeptly reconstructs graph G based on \mathbf{z} and the incomplete graph G' ; the encoder q is to depict the posterior distribution of \mathbf{z} . The hyper-parameter α functions as a balancing factor. See detailed derivation in A.2 in the appendix. During training, DIG-MILP modifies one constraint of an instance at a time. During inference, the graph rebuilt after removing a constraint can be fed back as input, allowing iterative modifications to the original data. The number of iterations controls the degree of structural similarity to the original problem. The inference procedure is shown in Algorithm. 2, where $\gamma|\mathcal{C}$ denotes the number of iterations to remove a constraint.

Neural Network Architecture For both the encoder and decoder, we employ the same bipartite graph neural networks (GNN) as the backbone. The encoder is as follows:

$$q_\phi(\mathbf{z}|G) = \prod_{u \in \mathcal{C} \cup \mathcal{V}} q_\phi(\mathbf{z}_u|G), \quad q_\phi(\mathbf{z}_u|G) = \mathcal{N}(\mu_\phi(\mathbf{h}_u^G), \Sigma_\phi(\mathbf{h}_u^G)), \quad (7)$$

where \mathbf{z}_u is conditionally independent with each other on G , $\mathbf{h}^G = \text{GNN}_\phi(G)$ denotes the node embeddings of G outputted by the encoder backbone, μ_ϕ and Σ_ϕ are two MLP layers that produce the mean and variance

for the distribution of \mathbf{z} . The decoder connects seven parts conditionally independent on the latent variable and node representations, with detailed structure as follows:

$$p_\theta(G|G', \mathbf{z}) = p_\theta(d_{c_i}|\mathbf{h}_{c_i}^{G'}, \mathbf{z}_{c_i}) \cdot \prod_{u \in \mathcal{V}} p_\theta(e(c_i, u)|\mathbf{h}_{c_i}^{G'}, \mathbf{z}_{c_i}) \cdot \prod_{u \in \mathcal{V}: e(c_i, u)=1} p_\theta(w_{c_i}|\mathbf{h}_{c_i}^{G'}, \mathbf{z}_{c_i}) \cdot \prod_{u \in \mathcal{C}} p_\theta(\mathbf{y}_u|\mathbf{h}_u^{G'}, \mathbf{z}_{\mathcal{C}}) p_\theta(\mathbf{r}_u|\mathbf{h}_u^{G'}, \mathbf{z}_{\mathcal{C}}) \cdot \prod_{u \in \mathcal{V}} p_\theta(\mathbf{x}_u|\mathbf{h}_u^{G'}, \mathbf{z}_{\mathcal{V}}) p_\theta(\mathbf{s}_u|\mathbf{h}_u^{G'}, \mathbf{z}_{\mathcal{V}}), \quad (8)$$

where $\mathbf{z}_{\mathcal{C}}, \mathbf{h}_{c_i}^{G'}$ denotes the latent variable and node representations on side \mathcal{C} , while $\mathbf{z}_{\mathcal{V}}, \mathbf{h}_{c_i}^{G'}$ signifies those on side \mathcal{V} ; d_{c_i} predicts the degree of the deleted node c_i ; $e(c_i, \cdot)$ denotes the probability of an edge between c_i and a node on side \mathcal{V} ; w_{c_i} is the edge weights connected with c_i ; $\mathbf{x}, \mathbf{y}, \mathbf{s}, \mathbf{r}$ are value of the solution and slacks. We use separate MLPs to model each part’s prediction as a regression task. We optimize each part of the decoder with the Huber Loss (Huber, 1992). See Section. B.2 in the appendix for more details.

Algorithm 1 DIG-MILP Training

Require: : dataset D , epoch N , batch size B

- 1: Solve MILPs for $\{[\mathbf{x}, \mathbf{y}, \mathbf{s}, \mathbf{r}]\}$ over D
- 2: Encode MILPs into graphs $\{G(\mathcal{V}, \mathcal{C}, \mathcal{E})\}$
- 3: **for** epoch=1,...,N **do**
- 4: Allocate empty batch $\mathcal{B} \leftarrow \emptyset$
- 5: **for** idx=1,...,B **do**
- 6: $G \sim D; G' \sim p(G'|G)$
- 7: $\mathcal{B} \leftarrow \mathcal{B} \cup \{(G, G')\}$
- 8: Encode $\mathbf{z} \sim q_\phi(\mathbf{z}|G)$
- 9: Decode $G \sim p_\theta(G|G', \mathbf{z})$
- 10: Calculate $\mathcal{L}_{\theta, \phi}(G, G')$
- 11: **end for**
- 12: $\mathcal{L}_{\theta, \phi} \leftarrow \frac{1}{B} \sum_{(G, G') \in \mathcal{B}} \mathcal{L}_{\theta, \phi}(G, G')$
- 13: Update ϕ, θ by minimizing $\mathcal{L}_{\theta, \phi}$
- 14: **end for**
- 15: **return** θ, ϕ

Algorithm 2 DIG-MILP Inference

Require: : dataset D , batch size B , constraint replace rate γ

- 1: Solve MILPs for $\{[\mathbf{x}, \mathbf{y}, \mathbf{s}, \mathbf{r}]\}$ over D
- 2: Encode MILPs into graphs $\{G(\mathcal{V}, \mathcal{C}, \mathcal{E})\}$
- 3: Allocate empty batch $\mathcal{B} \leftarrow \emptyset$
- 4: **for** id=1,...,B **do**
- 5: $G \sim D$
- 6: **for** t=1,..., $\gamma|\mathcal{C}|$ **do**
- 7: $G' \sim p(G'|G)$
- 8: $\mathbf{z} \sim \mathcal{N}(0, I)$
- 9: Decode $\tilde{G} \sim p_\theta(\tilde{G}|G', \mathbf{z})$
- 10: $G \leftarrow \tilde{G}$
- 11: **end for**
- 12: $\mathcal{B} \leftarrow \mathcal{B} \cup G$
- 13: **end for**
- 14: **return** new instance batch \mathcal{B}

4 Numerical Evaluations

In this section, we first delineate the experimental setup. Then we calculate the structural statistical similarity between generated and original instances. Subsequently, we evaluate DIG-MILP with two downstream tasks: (i) MILP data sharing for solver tuning and (ii) MILP data augmentation for ML model training.

4.1 Settings

Datasets: We perform DIG-MILP on four MILP datasets, encompassing scenarios involving simple and complex instances, a mix of small and large problem scales, varying instance quantities, and generation/collection from both synthetic and real-world sources. Specifically, we include two manually generated datasets, namely the set covering (SC) and the combinatorial auctions (CA), following the generation methodologies outlined in (Gasse et al., 2019). The remaining two datasets, namely CVS and IIS, are from the MIPLIB2017 benchmark (Gleixner et al., 2021)⁴, which comprises challenging instances from a large pool of problem-solving contexts. CVS pertains to the capacitated vertex separator problem on hypergraphs, while IIS mirrors real-world scenarios and resembles the set covering problems. Details are elaborated in Table. 2. It’s worth emphasizing that for CVS and IIS, we exclusively employ the ‘training’ data during the training of DIG-MILP and all downstream models. The ‘testing’ data is used only for downstream task evaluation.

Downstream Tasks: We devise two downstream applications, tailored to address distinct motivations. One motivation pertains to generating and sharing data that can substitute target instances. The other motivation involves data augmentation for better training ML models.

⁴https://miplib.zib.de/tag_benchmark.html

Table 2: Datasets Meta-data. For CVS and IIS, ‘training’ (non-bold) instances are for DIG-MILP or downstream model training, ‘testing’ (bold) instances are used in downstream testing only.

	SC	CA	CVS					IIS	
# data	1000	1000	training			testing		training	testing
			cvs08r139-94	cvs16r70-62	cvs16r89-60	cvs16r106-72	cvs16r128-89	iis-glass-cov	iis-hc-cov
# variable	400	300	1864	2112	2384	2848	3472	214	297
# constraint	200	$\sim 10^2$	2398	3278	3068	3608	4633	5375	9727
difficulty	easy	easy	hard					hard	

(S1): *Generating New Data for Solver Configuration Tuning* Through this part of experiment, we offer clients a potential approach and feasible research direction for attempting to utilize deep generative models to generate new instances and hand them over to companies specializing in MILP solver tuning. In particular, we calculate the Pearson positive correlation of the solution times required by the SCIP (Bestuzheva et al., 2021) solver between the generated examples and the original testing data across various hyper-parameter configurations. Should the solution time consistently demonstrate a positive correlation between the original and generated problems across varied parameter settings, it implies a consistent level of the effectiveness on the original and new instances under the same parameter configuration, which facilitates sharing data for parameter tuning.

(S2): *Optimal Value Prediction via ML* We train GNNs to express the optimum of the objective function in an MILP (Chen et al., 2023; 2024), which serves as an important proxy task to test NN’s ability in solving MILP instances. We follow exactly the experiment settings of Chen et al. (2023; 2024). The only difference is that instead of picking synthetic MILP problems as in Chen et al. (2023), we formulate more complicated and challenging datasets into MILP problems. We use the instances generated by DIG-MILPas data augmentation. For more detailed implementation, see B.6 in the appendix.

Solvers and Baselines: We use the open source solver SCIP (Bestuzheva et al., 2021) with its Python interface, namely PySCIPOpt (Maher et al., 2016b) for all the experiments. We consider two approaches as our baselines. The first, named ‘Bowly’, aligns with Bowly (2019) that generates MILP instances from scratch by sampling in an embedding space based on manually designed distributions, which to the best of our knowledge, is the only existing methods that work for generating novel MILP instances. The second baseline ‘random’ randomizes the network’s outputs, further validating the importance and efficacy of model training. For more implementation details of the baselines, please refer to B.3 in the appendix.

4.2 Results and Analysis

It’s shown that the instances generated by DIG-MILP share higher similarity with the original instance structures compared to baselines, for the statistical structural evaluation between the generated instances and the original instances, please refer to Appendix. B.4 for implementation details and C.1 for results.

4.2.1 downstream task #1: Generating New Data for Solver Configuration Tuning

We conduct experiments across all the four datasets. SCIP boasts an extensive array of parameters, rendering a tuning across the entire range impractical. Therefore, we adopt the reduced parameter space consistent with mainstream research on SCIP solver tuning (Hutter et al., 2011; Lindauer & Hutter, 2018; Lindauer et al., 2022). See Table. 11 in the appendix for detailed parameter space selection. We employ random seed 0 – 44 to generate 45 distinct parameter configurations. To validate the impact of randomness on SCIP, we initiate two independent trials on the same original testing data and compare the Pearson score of solution time. As illustrated in the diagonal of Table. 3, it clearly demonstrates a very high positive correlation for two independent trials on the same data. For subsequent experiments, each is run three times independently, with results averaged to mitigate randomness effects. We then compare the correlation of solution time on the original data across different datasets, as presented in the upper triangle of Table. 3. We observe a certain degree of positive correlation between synthetic datasets SC and CA, as well as between MIPLIB datasets CVS and IIS, which reveals that the effectiveness of parameters may naturally exhibit some degree of generalization across similar problems. However, the correlation between synthetic and MIPLIB datasets

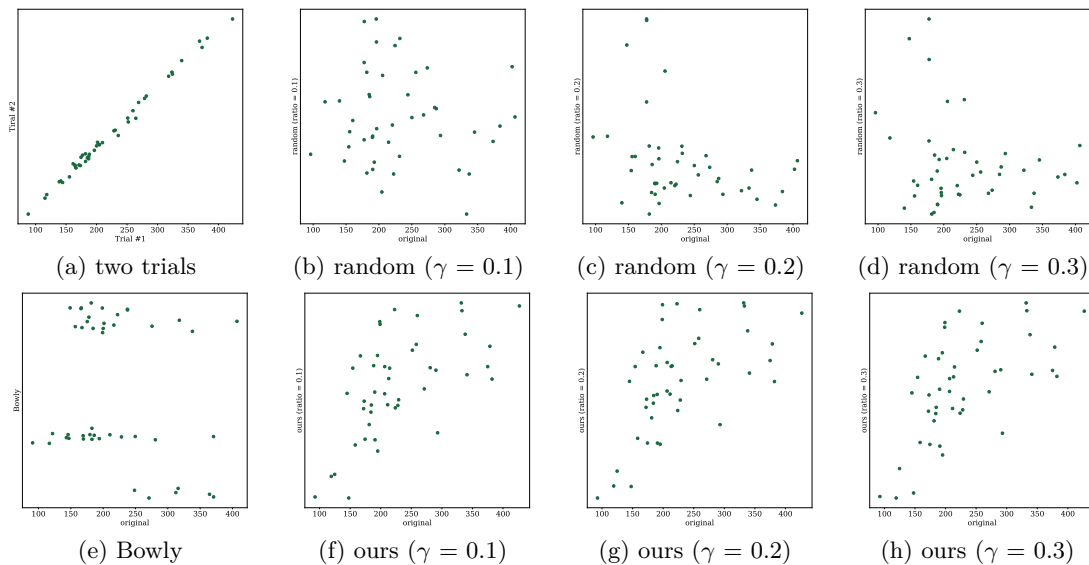


Figure 4: The solution time (second) of SCIP on CVS with 45 different hyper-parameter sets.

Table 3: The Pearson correlation coefficient (‘r’) and the significance value (‘p’) of the SCIP solution time under 45 different hyper-parameters on dataset-pairs.

		SC	CA	CVS	IIS
SC	r	0.732	0.599	0.115	0.088
	p	1.058e-8	1.351e-5	0.449	0.561
CA	r	-	0.952	0.021	0.092
	p	-	0.762e-24	0.890	0.545
CVS	r	-	-	0.997	0.550
	p	-	-	4.723e-53	9.033e-5
IIS	r	-	-	-	0.988
	p	-	-	-	1.563e-36

tends to be much lower, underscoring the necessity of generating new instances for solver tuning on specific problems. Finally, we compare the positive correlation of solution time between the generated instances and the original testing instances of the same datasets, as shown in Table. 4. Across all four datasets, the DIG-MILP-generated instances, exhibit the highest correlation with the testing data compared to the baselines, with the lowest p-value of significance. The correlation between solution times for real and synthetic instances was lower for the CVS and IIS datasets compared to CA and SC. This difference primarily stems from the availability of training data: CA and SC each had substantial training data, with 1000 instances for each task, while CVS and IIS, which are derived from MIPLIB, had significantly fewer instances (CVS had only 3 and IIS had just 1 for training). Generating synthetic instances from the given data requires capturing the underlying distribution information, which is typically more challenging when working with limited samples.

We visualize the correlation of solution time between the original testing data and the generated data on the CVS in Figure. 4. More detailed implementation and the visualization of the other datasets can be found in B.5 and Figure. 5-8 in the appendix.

4.2.2 downstream task #2: Optimal Value Prediction via machine learning

We conduct experiments for the second downstream task on all four datasets. It is important to note that the dataset used to train the DIG-MILP model for generating new samples is the same dataset used to train the neural network for optimal value prediction without data augmentation. This ensures that the DIG-MILP model is not exposed to any additional data beyond what the neural network receives, thereby maintaining the fairness of the experiment.

Table 4: The Pearson correlation coefficient (‘r’) and the significance value (‘p’) of the SCIP solution time between generated data and the original testing data under 45 different hyper-parameters on the SC, CA, CVS, and IIS problems.

		CA			SC			CVS			IIS		
Bowly	r	-0.048			0.683			-0.158			0.292		
	p	0.751			2.295e-7			0.298			0.051		
ratio		0.10	0.20	0.30	0.10	0.20	0.30	0.10	0.20	0.30	0.10	0.20	0.30
random	r	0.723	0.563	0.515	0.542	0.568	0.609	-0.085	-0.337	-0.201	0.114	0.182	0.149
	p	1.971e-8	5.522e-5	2.942e-4	1.174e-4	4.535e-5	9.028e-6	0.578	0.023	0.184	0.452	0.228	0.327
ours	r	0.728	0.771	0.780	0.747	0.717	0.665	0.609	0.590	0.607	0.542	0.300	0.551
	p	1.446e-8	5.371e-10	2.544e-10	3.646e-9	2.908e-8	6.353e-7	8.834e-6	1.986e-5	9.581e-6	1.187e-4	0.044	8.497e-5

Table 5: The relative mean square error (MSE) of the optimal objective value task on the set covering (SC) problem. The 500 original instances in training dataset #2 – #14 are identical.

dataset	#original	#generated	replace ratio	out-of-distribution				in-distribution				
				0.03	0.04	0.05	0.10	0.15	0.20	0.25	0.30	0.35
1	1000	0	-	0.792	0.640	0.488	0.022	0.009	0.009	0.010	0.011	0.015
2	500	500 (Bowly)	-	3.498	17.671	43.795	81.408	0.037	0.052	0.052	0.065	0.045
3	500	500 (random)	0.10	0.449	4.176	12.624	86.592	0.048	0.064	0.053	0.069	0.045
4	500	500 (DIG-MILP)	0.01	0.505	0.280	0.142	0.032	0.032	0.040	0.044	0.044	0.040
5	500	500 (DIG-MILP)	0.05	0.575	0.329	0.155	0.080	0.036	0.044	0.046	0.056	0.056
6	500	500 (DIG-MILP)	0.10	0.362	0.141	0.045	0.065	0.017	0.012	0.012	0.010	0.015
7	500	500 (DIG-MILP)	0.20	0.625	0.418	0.265	0.034	0.059	0.083	0.077	0.099	0.069
8	500	500 (DIG-MILP)	0.50	0.884	0.822	0.769	0.285	0.017	0.025	0.033	0.047	0.032
9	500	0	-	0.868	0.758	0.637	0.072	0.016	0.014	0.014	0.017	0.027
10	500	50 (DIG-MILP)	0.10	0.693	0.497	0.327	0.031	0.035	0.039	0.046	0.039	0.052
11	500	100 (DIG-MILP)	0.10	0.603	0.361	0.179	0.096	0.031	0.033	0.038	0.042	0.038
12	500	200 (DIG-MILP)	0.10	0.628	0.396	0.215	0.086	0.038	0.035	0.039	0.043	0.039
13	500	500 (DIG-MILP)	0.10	0.362	0.141	0.045	0.065	0.017	0.012	0.012	0.010	0.015
14	500	1000 (DIG-MILP)	0.10	0.473	0.211	0.063	0.339	0.013	0.014	0.014	0.014	0.024

Set Covering (SC) We select ‘density’ as a metric of the SC instance distribution, which represents the number of sets to be covered within a constraint. We only include densities ranging from 0.15 to 0.35 in the training set (for both DIG-MILP and the downstream predictor). We present in-distribution test set (0.15 to 0.35) as well as out-of-distribution test sets with densities falling within the unexplored range of 0.03 to 0.10, to reflect the predictor’s ability to generalize across distribution shift. The relative mean squared error (MSE) values of the models’ predictions are presented in Table. 5. In the upper rows (Datasets #1-#8), we fix the size of training set as 1000. Dataset #1 consist of 1000 original data, dataset #2 consists 500 original with 500 instances generated via the ‘Bowly’, #3 uses the ‘random’ baseline. Datasets #4-#8 comprise a combination of 500 original instances and 500 DIG-MILP-generated instances, with various constraint node replacement ratios γ ranging from 0.01 to 0.50. Models trained exclusively on in-distribution data exhibit superior fitting and predictive accuracy within the in-distribution test sets. However, models trained on a combination of original and DIG-MILP-generated instances display significantly enhanced prediction accuracy on out-of-distribution testing data. We attribute this phenomenon to the increased structural and label diversity in the newly generated instances, mitigating over-fitting on in-distribution data and consequently bolstering the model’s cross-distribution capabilities. It’s worth noting that ‘Bowly’ or ‘random’ neither enhances the model’s in-distribution nor out-of-distribution performance. We believe this is due to the less precise representation of the target distribution by the manually-designed ‘Bowly’ baseline and the excessively high randomness in ‘random’, causing the generated instances to deviate substantially from the original problems in both solution space and structure. In the lower rows (Datasets #9-#14), we investigate the impact of progressively incorporating DIG-MILP-generated instances into the dataset, initially starting with 500 original instances. We observe a consistent improvement in model performance with the gradual inclusion of additional newly generated instances, with peak performance achieved when augmenting the dataset with 500 newly generated instances.

Combinatorial Auctions (CA) We set the number of bid/item pairs that determines the quantity of variables and constraints as the parameter for distribution shift. Our training set only comprises examples with bid/item values ranging from 40/200 to 80/400, our testing set also introduces instances with bid/item values ranging from 40/200 to 160/800. The relative mean squared error (MSE) of the model’s predictions

Table 6: The relative mean square error (MSE) of the optimal objective value task on the combinatorial auction (CA) problem. The 500 original instances in training dataset #2 – #14 are identical.

dataset	#original	#generated	replace ratio	in-distribution			out-of-distribution			
				40/200	60/300	80/400	100/500	120/600	140/700	160/800
1	1000	0	-	0.246	0.003	0.060	0.155	0.239	0.312	0.379
2	500	500 (Bowly)	-	0.202	0.004	0.080	0.183	0.272	0.346	0.410
3	500	500 (random)	0.10	0.242	0.006	0.077	0.179	0.269	0.347	0.409
4	500	500 (DIG-MILP)	0.01	0.346	0.008	0.043	0.131	0.219	0.292	0.359
5	500	500 (DIG-MILP)	0.05	0.345	0.009	0.041	0.125	0.211	0.284	0.352
6	500	500 (DIG-MILP)	0.10	0.385	0.015	0.036	0.118	0.201	0.276	0.340
7	500	500 (DIG-MILP)	0.20	0.428	0.019	0.035	0.116	0.203	0.275	0.344
8	500	500 (DIG-MILP)	0.30	0.381	0.012	0.040	0.126	0.215	0.289	0.356
9	500	500 (DIG-MILP)	0.50	0.398	0.014	0.035	0.117	0.203	0.276	0.344
10	500	0	-	0.216	0.004	0.068	0.165	0.249	0.324	0.388
11	500	50 (DIG-MILP)	0.10	0.382	0.006	0.040	0.130	0.218	0.293	0.361
12	500	100 (DIG-MILP)	0.10	0.446	0.014	0.031	0.116	0.201	0.275	0.344
13	500	500 (DIG-MILP)	0.10	0.385	0.015	0.036	0.118	0.201	0.276	0.340
14	500	1000 (DIG-MILP)	0.10	0.359	0.009	0.039	0.126	0.212	0.285	0.351

is provided in Table. 6. The experiments are also divided into two parts. The upper rows (Datasets #1-#8) yields similar conclusions, where models trained solely on original data excel in fitting within in-distribution test sets, models trained on a mixture of half original and half DIG-MILP-generated instances perform better on test sets at scales never encountered during training (bid/item ranging from 100/500 to 160/800). This observation is attributed to the diversity introduced by the generated instances, in terms of both the problem structure and optimal objective labels, that prevents the models from over-fitting and thereby enhance their generalization across scales. Consistent with the SC, the second part demonstrates the impact of gradually increasing the new instances as training data and also achieves the peak performance with 500 newly generated instances.

CVS and IIS Experiments on CVS and IIS show similar insights, see Appendix. C.2 for details.

5 Conclusion

This paper introduces DIG-MILP, a deep generative framework for MILP. Contrasting with conventional MILP generation techniques, DIG-MILP does not rely on domain-specific expertise. Instead, it employs DNNs to extract profound structural information from limited MILP data, generating “representative” instances. Notably, DIG-MILP guarantees the feasibility and boundedness of generated data, ensuring the data’s “authenticity”. The generation space of DIG-MILP encompasses any feasible-bounded MILP, making it a general framework for generating feasible-bounded MILPs. Experiment evaluations highlights DIG-MILP’s potential in (S1) MILP data sharing for solver hyper-parameter tuning without publishing the original data and (S2) data augmentation to enhance the generalization capacity of ML models tasked with solving MILPs. As infeasible or unbounded problems are also important, particularly in testing the robustness of MILP solvers. Therefore, exploring the generation of these types of instances represents a promising direction for future research.

References

- Tobias Achterberg and Roland Wunderling. Mixed integer programming: Analyzing 12 years of progress. In *Facets of combinatorial optimization: Festschrift for martin grötschel*, pp. 449–481. Springer, 2013.
- Naser Al-Falahy and Omar Y Alani. Technologies for 5g networks: Challenges and opportunities. *It Professional*, 19(1):12–20, 2017.
- Yuihci Asahiro, Kazuo Iwama, and Eiji Miyano. Random generation of test instances with controlled attributes. *Cliques, Coloring, and Satisfiability*, pp. 377–393, 1996.
- Egon Balas and Andrew Ho. *Set covering algorithms using cutting planes, heuristics, and subgradient optimization: a computational study*. Springer, 1980.

- Yoshua Bengio, Nicholas Léonard, and Aaron Courville. Estimating or propagating gradients through stochastic neurons for conditional computation. *arXiv preprint arXiv:1308.3432*, 2013.
- Dimitris Bertsimas and John N Tsitsiklis. *Introduction to linear optimization*, volume 6. Athena scientific Belmont, MA, 1997.
- Ksenia Bestuzheva, Mathieu Besançon, Wei-Kun Chen, Antonia Chmiela, Tim Donkiewicz, Jasper van Doornmalen, Leon Eifler, Oliver Gaul, Gerald Gamrath, Ambros Gleixner, et al. The scip optimization suite 8.0. *arXiv preprint arXiv:2112.08872*, 2021.
- Simon Bowly, Kate Smith-Miles, Davaatseren Baatar, and Hans Mittelmann. Generation techniques for linear programming instances with controllable properties. *Mathematical Programming Computation*, 12(3):389–415, 2020.
- Simon Andrew Bowly. *Stress testing mixed integer programming solvers through new test instance generation methods*. PhD thesis, School of Mathematical Sciences, Monash University, 2019.
- Juergen Branke, Su Nguyen, Christoph W Pickardt, and Mengjie Zhang. Automated design of production scheduling heuristics: A review. *IEEE Transactions on Evolutionary Computation*, 20(1):110–124, 2015.
- Aykut Bulut and Ted K Ralphs. On the complexity of inverse mixed integer linear optimization. *SIAM Journal on Optimization*, 31(4):3014–3043, 2021.
- Richard H Byrd, Alan J Goldman, and Miriam Heller. Recognizing unbounded integer programs. *Operations Research*, 35(1):140–142, 1987.
- Ziang Chen, Jialin Liu, Xinshang Wang, Jianfeng Lu, and Wotao Yin. On representing linear programs by graph neural networks. *International Conference on Learning Representations*, 2023.
- Ziang Chen, Jialin Liu, Xiaohan Chen, Xinshang Wang, and Wotao Yin. Rethinking the capacity of graph neural networks for branching strategy. *arXiv preprint arXiv:2402.07099*, 2024.
- Michele Conforti, Gérard Cornuéjols, Giacomo Zambelli, Michele Conforti, Gérard Cornuéjols, and Giacomo Zambelli. *Integer programming models*. Springer, 2014.
- IBM ILOG Cplex. V12. 1: User’s manual for cplex. *International Business Machines Corporation*, 46(53):157, 2009.
- Antonia Creswell, Tom White, Vincent Dumoulin, Kai Arulkumaran, Biswa Sengupta, and Anil A Bharath. Generative adversarial networks: An overview. *IEEE signal processing magazine*, 35(1):53–65, 2018.
- J Culberson. A graph generator for various classes of k-colorable graphs. URL <http://webdocs.cs.ualberta.ca/~joe/Coloring/Generators/generate.html>, 2002.
- Mădălina M Drugan. Instance generator for the quadratic assignment problem with additively decomposable cost function. In *2013 IEEE Congress on Evolutionary Computation*, pp. 2086–2093. IEEE, 2013.
- Matthias Fey and Jan Eric Lenssen. Fast graph representation learning with pytorch geometric. *arXiv preprint arXiv:1903.02428*, 2019.
- Gerald Gamrath, Thorsten Koch, Alexander Martin, Matthias Miltenberger, and Dieter Weninger. Progress in presolving for mixed integer programming. *Mathematical Programming Computation*, 7:367–398, 2015.
- Maxime Gasse, Didier Chételat, Nicola Ferroni, Laurent Charlin, and Andrea Lodi. Exact combinatorial optimization with graph convolutional neural networks. *Advances in neural information processing systems*, 32, 2019.
- Zijie Geng, Xijun Li, Jie Wang, Xiao Li, Yongdong Zhang, and Feng Wu. A deep instance generative framework for milp solvers under limited data availability. *Advances in Neural Information Processing Systems*, 36, 2024.

- Ambros Gleixner, Gregor Hendel, Gerald Gamrath, Tobias Achterberg, Michael Bastubbe, Timo Berthold, Philipp Christophel, Kati Jarck, Thorsten Koch, Jeff Linderoth, et al. Miplib 2017: data-driven compilation of the 6th mixed-integer programming library. *Mathematical Programming Computation*, 13(3): 443–490, 2021.
- Gurobi. Gurobi Optimizer Reference Manual, 2023. URL <https://www.gurobi.com>.
- Juris Hartmanis. Computers and intractability: a guide to the theory of np-completeness (michael r. garey and david s. johnson). *Siam Review*, 24(1):90, 1982.
- R Hill, JT Moore, C Hiremath, and YK Cho. Test problem generation of binary knapsack problem variants and the implications of their use. *Int. J. Oper. Quant. Manag.*, 18(2):105–128, 2011.
- Raymond R Hill and Charles H Reilly. The effects of coefficient correlation structure in two-dimensional knapsack problems on solution procedure performance. *Management Science*, 46(2):302–317, 2000.
- Jonathan Ho, Ajay Jain, and Pieter Abbeel. Denoising diffusion probabilistic models. *Advances in neural information processing systems*, 33:6840–6851, 2020.
- John N Hooker. Needed: An empirical science of algorithms. *Operations research*, 42(2):201–212, 1994.
- John N Hooker. Testing heuristics: We have it all wrong. *Journal of heuristics*, 1:33–42, 1995.
- Peter J Huber. Robust estimation of a location parameter. In *Breakthroughs in statistics: Methodology and distribution*, pp. 492–518. Springer, 1992.
- Michael H Hugos. *Essentials of supply chain management*. John Wiley & Sons, 2018.
- Frank Hutter, Holger H Hoos, and Kevin Leyton-Brown. Sequential model-based optimization for general algorithm configuration. In *Learning and Intelligent Optimization: 5th International Conference, LION 5, Rome, Italy, January 17-21, 2011. Selected Papers 5*, pp. 507–523. Springer, 2011.
- Eric Jang, Shixiang Gu, and Ben Poole. Categorical reparameterization with gumbel-softmax. *arXiv preprint arXiv:1611.01144*, 2016.
- Richard M Karp. *Reducibility among combinatorial problems*. Springer, 2010.
- Elias Khalil, Pierre Le Bodic, Le Song, George Nemhauser, and Bistra Dilkina. Learning to branch in mixed integer programming. In *Proceedings of the AAAI Conference on Artificial Intelligence*, volume 30, 2016.
- Elias Khalil, Hanjun Dai, Yuyu Zhang, Bistra Dilkina, and Le Song. Learning combinatorial optimization algorithms over graphs. *Advances in neural information processing systems*, 30, 2017.
- Diederik P Kingma and Jimmy Ba. Adam: A method for stochastic optimization. *arXiv preprint arXiv:1412.6980*, 2014.
- Diederik P Kingma and Max Welling. Auto-encoding variational bayes. *arXiv preprint arXiv:1312.6114*, 2013.
- Thomas N Kipf and Max Welling. Variational graph auto-encoders. *arXiv preprint arXiv:1611.07308*, 2016.
- Eugene L Lawler and David E Wood. Branch-and-bound methods: A survey. *Operations research*, 14(4): 699–719, 1966.
- Marius Lindauer and Frank Hutter. Warmstarting of model-based algorithm configuration. In *Proceedings of the AAAI Conference on Artificial Intelligence*, volume 32, 2018.
- Marius Lindauer, Katharina Eggenberger, Matthias Feurer, André Biedenkapp, Difan Deng, Carolin Benjamins, Tim Ruhkopf, René Sass, and Frank Hutter. Smac3: A versatile bayesian optimization package for hyperparameter optimization. *The Journal of Machine Learning Research*, 23(1):2475–2483, 2022.

- Han Lu, Zenan Li, Runzhong Wang, Qibing Ren, Xijun Li, Mingxuan Yuan, Jia Zeng, Xiaokang Yang, and Junchi Yan. Roco: A general framework for evaluating robustness of combinatorial optimization solvers on graphs. In *The Eleventh International Conference on Learning Representations*, 2022.
- Chris J Maddison, Andriy Mnih, and Yee Whye Teh. The concrete distribution: A continuous relaxation of discrete random variables. *arXiv preprint arXiv:1611.00712*, 2016.
- Stephen Maher, Matthias Miltenberger, João Pedro Pedroso, Daniel Rehfeldt, Robert Schwarz, and Felipe Serrano. PySCIPOpt: Mathematical programming in python with the SCIP optimization suite. In *Mathematical Software – ICMS 2016*, pp. 301–307. Springer International Publishing, 2016a. doi: 10.1007/978-3-319-42432-3_37.
- Stephen Maher, Matthias Miltenberger, João Pedro Pedroso, Daniel Rehfeldt, Robert Schwarz, and Felipe Serrano. Pyscipopt: Mathematical programming in python with the scip optimization suite. In *Mathematical Software–ICMS 2016: 5th International Conference, Berlin, Germany, July 11-14, 2016, Proceedings 5*, pp. 301–307. Springer, 2016b.
- Renata Mansini, odzimierz Ogryczak WŁ, M Grazia Speranza, and EURO: The Association of European Operational Research Societies. *Linear and mixed integer programming for portfolio optimization*, volume 21. Springer, 2015.
- Robert R Meyer. On the existence of optimal solutions to integer and mixed-integer programming problems. *Mathematical Programming*, 7:223–235, 1974.
- Vinod Nair, Sergey Bartunov, Felix Gimeno, Ingrid Von Glehn, Pawel Lichocki, Ivan Lobov, Brendan O’Donoghue, Nicolas Sonnerat, Christian Tjandraatmadja, Pengming Wang, et al. Solving mixed integer programs using neural networks. *arXiv preprint arXiv:2012.13349*, 2020.
- Adam Paszke, Sam Gross, Francisco Massa, Adam Lerer, James Bradbury, Gregory Chanan, Trevor Killeen, Zeming Lin, Natalia Gimelshein, Luca Antiga, et al. Pytorch: An imperative style, high-performance deep learning library. *Advances in neural information processing systems*, 32, 2019.
- Martha G Pilcher and Ronald L Rardin. Partial polyhedral description and generation of discrete optimization problems with known optima. *Naval Research Logistics (NRL)*, 39(6):839–858, 1992.
- Ilija Radosavovic, Raj Prateek Kosaraju, Ross Girshick, Kaiming He, and Piotr Dollár. Designing network design spaces. In *Proceedings of the IEEE/CVF conference on computer vision and pattern recognition*, pp. 10428–10436, 2020.
- Arthur Richards and Jonathan P How. Aircraft trajectory planning with collision avoidance using mixed integer linear programming. In *Proceedings of the 2002 American Control Conference (IEEE Cat. No. CH37301)*, volume 3, pp. 1936–1941. IEEE, 2002.
- Ismael Rodríguez, Fernando Rubio, and Pablo Rabanal. Automatic media planning: optimal advertisement placement problems. In *2016 IEEE Congress on Evolutionary Computation (CEC)*, pp. 5170–5177. IEEE, 2016.
- Paul C Roling, Hendrikus G Visser, et al. Optimal airport surface traffic planning using mixed-integer linear programming. *International Journal of Aerospace Engineering*, 2008, 2008.
- Alexander Schrijver. *Theory of linear and integer programming*. John Wiley & Sons, 1998.
- Kate Smith-Miles and Simon Bowly. Generating new test instances by evolving in instance space. *Computers & Operations Research*, 63:102–113, 2015.
- Yang Song and Stefano Ermon. Generative modeling by estimating gradients of the data distribution. *Advances in neural information processing systems*, 32, 2019.
- Russ J Vander Wiel and Nikolaos V Sahinidis. Heuristic bounds and test problem generation for the time-dependent traveling salesman problem. *Transportation Science*, 29(2):167–183, 1995.

Pauli Virtanen, Ralf Gommers, Travis E. Oliphant, Matt Haberland, Tyler Reddy, David Cournapeau, Evgeni Burovski, Pearu Peterson, Warren Weckesser, Jonathan Bright, Stéfan J. van der Walt, Matthew Brett, Joshua Wilson, K. Jarrod Millman, Nikolay Mayorov, Andrew R. J. Nelson, Eric Jones, Robert Kern, Eric Larson, C J Carey, İlhan Polat, Yu Feng, Eric W. Moore, Jake VanderPlas, Denis Laxalde, Josef Perktold, Robert Cimrman, Ian Henriksen, E. A. Quintero, Charles R. Harris, Anne M. Archibald, Antônio H. Ribeiro, Fabian Pedregosa, Paul van Mulbregt, and SciPy 1.0 Contributors. SciPy 1.0: Fundamental Algorithms for Scientific Computing in Python. *Nature Methods*, 17:261–272, 2020. doi: 10.1038/s41592-019-0686-2.

Laurence A Wolsey. *Integer programming*. John Wiley & Sons, 2020.

A supplementary theoretical results

A.1 Proof of Proposition 1

To validate Proposition 1, we follow the methodology outlined in Bowly (2019). Before the proof of Proposition 1, we first give the definition of boundedness, feasibility and optimal solutions of MILP, then we discuss the existence of optimal solutions of LP and MILP.

Definition 1 (Feasibility of MILP). *An MILP($\mathbf{A}, \mathbf{b}, \mathbf{c}$) is feasible if there exists an \mathbf{x} such that all the constraints are satisfied: $\mathbf{x} \in \mathbb{Z}_{\geq 0}^n, \mathbf{A}\mathbf{x} \leq \mathbf{b}$. Such an \mathbf{x} is named a feasible solution.*

Definition 2 (Boundedness of MILP). *An MILP($\mathbf{A}, \mathbf{b}, \mathbf{c}$) is bounded if there's an upper bound on $\mathbf{c}^\top \mathbf{x}$ across all feasible solutions.*

Definition 3 (Optimal Solution for MILP). *A vector \mathbf{x}^* is recognized as an optimal solution if it's a feasible solution and it is no worse than all other feasible solutions: $\mathbf{c}^\top \mathbf{x}^* \geq \mathbf{c}^\top \mathbf{x}$, given \mathbf{x} is feasible.*

All LPs must fall into one of the following cases Bertsimas & Tsitsiklis (1997):

- Infeasible.
- Feasible but unbounded.
- Feasible and bounded. Only in this case, the LP yields an optimal solution.

However, general MILP will be much more complicated. Consider a simple example: $\min \sqrt{3}x_1 - x_2$, s.t. $\sqrt{3}x_1 - x_2 \geq 0, x_1 \geq 1, \mathbf{x} \in \mathbb{Z}_{\geq 0}^2$. No feasible solution has objective equal to zero, but there are feasible solutions with objective arbitrarily close to zero. In other words, *an MILP might be bounded but with no optimal solutions*. Such a pathological phenomenon is caused by the irrational number $\sqrt{3}$ in the coefficient. Therefore, we only consider MILP with rational data:

$$\mathbf{A} \in \mathbb{Q}^{m \times n}, \mathbf{b} \in \mathbb{Q}^m, \mathbf{c} \in \mathbb{Q}^m.$$

Such an assumption is regularly adopted in the research of MILP.

Without requiring \mathbf{x} to be integral, equation 1 will be relaxed to an LP, named its *LP relaxation*:

$$\mathbf{LP}(\mathbf{A}, \mathbf{b}, \mathbf{c}) : \max_{\mathbf{x}} \mathbf{c}^\top \mathbf{x}, \quad \text{s.t. } \mathbf{A}\mathbf{x} \leq \mathbf{b}, \mathbf{x} \geq 0.$$

The feasibility, boundedness, and existence of optimal solutions, along with the relationship with its LP relaxation, are summarized in the following lemma.

Lemma 1. *Given $\mathbf{A} \in \mathbb{Q}^{m \times n}, \mathbf{b} \in \mathbb{Q}^m, \mathbf{c} \in \mathbb{Q}^m$, it holds that*

- (I) *If LP($\mathbf{A}, \mathbf{b}, \mathbf{c}$) is infeasible, MILP($\mathbf{A}, \mathbf{b}, \mathbf{c}$) must be infeasible.*
- (II) *If LP($\mathbf{A}, \mathbf{b}, \mathbf{c}$) is feasible but unbounded, then MILP($\mathbf{A}, \mathbf{b}, \mathbf{c}$) must be either infeasible or unbounded.*
- (III) *If LP($\mathbf{A}, \mathbf{b}, \mathbf{c}$) is feasible and bounded, MILP($\mathbf{A}, \mathbf{b}, \mathbf{c}$) might be infeasible or feasible. If we further assume MILP($\mathbf{A}, \mathbf{b}, \mathbf{c}$) is feasible, it must yield an optimal solution.*

Proof. Conclusion (I) is trivial. Conclusion (II) is exactly (Byrd et al., 1987, Theorem 1). Conclusion (III) is a corollary of (Meyer, 1974, Theorem 2.1). To obtain (III), we first write MILP($\mathbf{A}, \mathbf{b}, \mathbf{c}$) into the following form:

$$\max_{\mathbf{x}, \mathbf{r}} \mathbf{c}^\top \mathbf{x} \quad \text{s.t. } \mathbf{A}\mathbf{x} + \mathbf{r} = \mathbf{b}, \mathbf{x} \geq \mathbf{0}, \mathbf{r} \geq \mathbf{0}, \mathbf{x} \text{ is integral}$$

Then the condition (v) in (Meyer, 1974, Theorem 2.1) can be directly applied. Therefore, the feasibility and boundedness of MILP($\mathbf{A}, \mathbf{b}, \mathbf{c}$) imply the existence of optimal solutions, which concludes the proof. \square

With Lemma 1, we could prove Proposition 1 now.

Proof of Proposition 1. At the beginning, we define the space of $[\mathbf{A}, \mathbf{b}, \mathbf{c}]$ generated based on \mathcal{F} as \mathcal{H}'' for simplicity.

$$\mathcal{H}'' := \left\{ [\mathbf{A}, \mathbf{b}, \mathbf{c}] : \mathbf{b} = \mathbf{A}\mathbf{x} + \mathbf{r}, \mathbf{c} = \mathbf{A}^\top \mathbf{y} - \mathbf{s}, [\mathbf{A}, \mathbf{x}, \mathbf{y}, \mathbf{s}, \mathbf{r}] \in \mathcal{F} \right\}$$

Then it's enough to show that $\mathcal{H}' \subset \mathcal{H}''$ and $\mathcal{H}'' \subset \mathcal{H}'$.

We first show $\mathcal{H}'' \subset \mathcal{H}'$: For any $[\mathbf{A}, \mathbf{b}, \mathbf{c}] \in \mathcal{H}''$, it holds that $[\mathbf{A}, \mathbf{b}, \mathbf{c}] \in \mathcal{H}'$. In another word, we have to show $\text{MILP}(\mathbf{A}, \mathbf{b}, \mathbf{c})$ to be feasible and bounded for all $[\mathbf{A}, \mathbf{b}, \mathbf{c}] \in \mathcal{H}''$. The feasibility can be easily verified. The boundedness can be proved by "weak duality." For the sake of completeness, we provide a detailed proof here. Define the Lagrangian as

$$\mathcal{L}(\mathbf{x}, \mathbf{y}) := \mathbf{c}^\top \mathbf{x} + \mathbf{y}^\top (\mathbf{b} - \mathbf{A}\mathbf{x})$$

Inequalities $\mathbf{A}\mathbf{x} \leq \mathbf{b}$ and $\mathbf{y} \geq \mathbf{0}$ imply

$$\mathcal{L}(\mathbf{x}, \mathbf{y}) \geq \mathbf{c}^\top \mathbf{x}$$

Inequalities $\mathbf{A}^\top \mathbf{y} \geq \mathbf{c}$ and $\mathbf{x} \geq \mathbf{0}$ imply

$$\mathcal{L}(\mathbf{x}, \mathbf{y}) \leq \mathbf{b}^\top \mathbf{y}$$

Since $\mathbf{x} \in \mathbb{Q}_{\geq 0}^n$ and $\mathbf{y} \in \mathbb{Q}_{\geq 0}^m$, it holds that

$$-\infty < \mathbf{c}^\top \mathbf{x} \leq \mathbf{b}^\top \mathbf{y} < +\infty$$

which concludes the boundedness of $\text{MILP}(\mathbf{A}, \mathbf{b}, \mathbf{c})$.

We then show $\mathcal{H}' \subset \mathcal{H}''$: For any $\text{MILP}(\mathbf{A}, \mathbf{b}, \mathbf{c})$ that is feasible and bounded, there must be $[\mathbf{A}, \mathbf{x}, \mathbf{y}, \mathbf{s}, \mathbf{r}] \in \mathcal{F}$ such that

$$\mathbf{b} = \mathbf{A}\mathbf{x} + \mathbf{r}, \tag{9}$$

$$\mathbf{c} = \mathbf{A}^\top \mathbf{y} - \mathbf{s}. \tag{10}$$

The existence of \mathbf{x}, \mathbf{r} , along with equation 9, is a direct conclusion of the feasibility of $\text{MILP}(\mathbf{A}, \mathbf{b}, \mathbf{c})$. Now let's prove the existence of rational vectors \mathbf{y}, \mathbf{s} , along with equation 10. Since $\text{MILP}(\mathbf{A}, \mathbf{b}, \mathbf{c})$ is feasible and bounded, according to Lemma 1, $\text{LP}(\mathbf{A}, \mathbf{b}, \mathbf{c})$ must be feasible and bounded. Thanks to the weak duality discussed above, we conclude that $\text{DualLP}(\mathbf{A}, \mathbf{b}, \mathbf{c})$ must be feasible and bounded. As long as $\text{DualLP}(\mathbf{A}, \mathbf{b}, \mathbf{c})$ has an optimal solution \mathbf{y}^* that is rational, one can obtain equation 10 by regarding $[\mathbf{y}^*, \mathbf{A}^\top \mathbf{y}^* - \mathbf{c}]$ as $[\mathbf{y}, \mathbf{s}]$. Therefore, it's enough to show $\text{DualLP}(\mathbf{A}, \mathbf{b}, \mathbf{c})$ has a rational optimal solution.

Define:

$$\mathbf{A}' = [\mathbf{A}^\top, -\mathbf{I}]$$

$$\mathbf{y}' = [\mathbf{y}^\top, \mathbf{s}^\top]^\top$$

$$\mathbf{b}' = [\mathbf{b}^\top, \mathbf{0}^\top]$$

Then DualLP can be written as a standard-form LP:

$$\min_{\mathbf{y}'} (\mathbf{b}')^\top \mathbf{y}' \quad \text{s.t.} \quad \mathbf{A}' \mathbf{y}' = \mathbf{c}, \mathbf{y}' \geq \mathbf{0} \tag{11}$$

As long as an LP has an optimal solution, it must have a basic optimal solution Bertsimas & Tsitsiklis (1997). Specifically, we can split \mathbf{A}' in column-based fashion as $\mathbf{A}' = [\mathbf{B}', \mathbf{N}']$ and split \mathbf{y}' as $\mathbf{y}' = [\mathbf{y}_B^\top, \mathbf{y}_N^\top]^\top$, where $\mathbf{y}_N = \mathbf{0}$. Such a \mathbf{y}' is termed a *basic optimal solution* to the LP presented in equation 11. Therefore,

$$\mathbf{A}' \mathbf{y}' = \mathbf{B}' \mathbf{y}_B + \mathbf{N}' \mathbf{y}_N = \mathbf{B}' \mathbf{y}_B = \mathbf{c} \implies \mathbf{y}_B = (\mathbf{B}')^{-1} \mathbf{c}$$

Since \mathbf{B}' is a sub-matrix of \mathbf{A}' , \mathbf{B}' is rational. Therefore, $(\mathbf{B}')^{-1}$ and \mathbf{y}_B are rational, which implies \mathbf{y}' is rational. This concludes the existence of rational optimal solutions of DualLP , which finishes the entire proof. \square

A.2 Derivation of the loss function

Here we show the derivation from the training objective in Equation. 5 towards the loss function in Equation. 6.

$$\begin{aligned}
\log \mathbb{P}(G|G'; \theta, \phi) &= \mathbb{E}_{\mathbf{z} \sim q_\phi(\mathbf{z}|G)} \log \mathbb{P}(G|G'; \theta, \phi) \\
&= \mathbb{E}_{\mathbf{z} \sim q_\phi(\mathbf{z}|G)} \left[\log \frac{p_\theta(G|G', \mathbf{z}) p(\mathbf{z})}{q_\phi(\mathbf{z}|G)} \frac{q_\phi(\mathbf{z}|G)}{p(\mathbf{z}|G)} \right] \\
&= \mathbb{E}_{\mathbf{z} \sim q_\phi(\mathbf{z}|G)} \log \frac{p_\theta(G|G', \mathbf{z}) p(\mathbf{z})}{q_\phi(\mathbf{z}|G)} + \mathbb{E}_{\mathbf{z} \sim q_\phi(\mathbf{z}|G)} \left[\log \frac{q_\phi(\mathbf{z}|G)}{p(\mathbf{z}|G)} \right], \quad (12) \\
&= \mathbb{E}_{\mathbf{z} \sim q_\phi(\mathbf{z}|G)} [\log p_\theta(G|\mathbf{z}, G')] - \mathcal{D}_{KL}[q_\phi(\mathbf{z}|G) \| p(\mathbf{z})] + \mathcal{D}_{KL}[q_\phi(\mathbf{z}|G) \| p(\mathbf{z}|G)] \\
&\geq \mathbb{E}_{\mathbf{z} \sim q_\phi(\mathbf{z}|G)} [\log p_\theta(G|G', \mathbf{z})] - \mathcal{D}_{KL}[q_\phi(\mathbf{z}|G) \| \mathcal{N}(0, I)]
\end{aligned}$$

and thus we have

$$\mathbb{E}_{G \sim \mathcal{G}} \mathbb{E}_{G' \sim p_{G'|G}} \log \mathbb{P}(G|G'; \theta, \phi) \geq -\mathcal{L}_{\theta, \phi} \quad (13)$$

B supplementary implementation details

B.1 Hardware, Software and Platforms

At the hardware level, we employ an Intel Xeon Gold 6248R CPU and a Nvidia quadro RTX 6000 GPU. For tasks that exclusively run on the CPU, we utilize a single core, for tasks that run on the GPU, we set the upper limit to 10 cores. On the software side, we utilize PyTorch version 2.0.0+cu117 (Paszke et al., 2019) and PyTorch Geometric version 2.0.3 (Fey & Lenssen, 2019). We utilize PySCIPOpt solver version 3.5.0 (Maher et al., 2016a) for optimization purposes with default configurations.

B.2 Implementation of DIG-MILP

For both the encoder and the decoder, we adopt the bipartite GNN exactly the same as that in Gasse et al. (2019) as their backbones, the original codes for the backbone is publicly available⁵.

Encoder To obtain the latent variable samples, we feed the encoder with G encoded as per the method in Table. 1, we then incorporate two distinct multi-layer perceptron (MLP) layers following the backbone to output the mean and log variance of the latent variable \mathbf{z} . During the training process, we use the re-parametrization trick (Bengio et al., 2013; Maddison et al., 2016; Jang et al., 2016) to render the process of sampling \mathbf{z} from the mean and variance differentiable. During inference, we directly sample $\mathbf{z} \sim \mathcal{N}(0, I)$.

Decoder We feed the backbone of the decoder with the incomplete graph G' to obtain the latent node representations $\mathbf{h}^{G'} = \{\mathbf{h}_e^{G'}, \mathbf{h}_v^{G'}\}$. The backbone is then followed by seven distinct heads conditionally independent on \mathbf{h} and \mathbf{z} , each corresponding to the prediction of: 1) the degree of the removed node d_{c_i} , 2) the edges $e(c_i, u)$ between the constraint node c_i and the nodes in the other side, 3) the edge weights w_{c_i} , and 4) - 7) the value of $\mathbf{x}, \mathbf{y}, \mathbf{r}, \mathbf{s}$ of the new graph \tilde{G} . Each head is composed of layers of MLP, and takes different combinations $\mathbf{h}^{G'}, \mathbf{z}^{G'}$ as inputs, which is illustrated in Table. 7. We perform min-max normalization on all the variables to predict according to their maximum and minimum value occurred in the training dataset. Each part is modeled as a regression task, where we use the Huber Loss Huber (1992) as the criterion for each part and add them together as the total loss for decoder.

Table 7: The last layer design of decoder.

prediction	embeddings
$d, e, w, \mathbf{x}, \mathbf{r}$	$\mathbf{h}_v, \mathbf{z}_v, v \in \mathcal{V}$
\mathbf{y}, \mathbf{s}	$\mathbf{h}_c, \mathbf{z}_c, c \in \mathcal{C}$

For the case of binary MILP problems, their primal, dual and slack variables could be written in the form as Equation. 14 15 16:

⁵<https://github.com/ds4dm/learn2branch/blob/master/models/baseline/model.py>

$$\begin{array}{ccc}
\textbf{Primal (Binary)} & \textbf{Dual (Binary)} & \textbf{Slack (Binary)} \\
\max_{\mathbf{x}} \mathbf{c}^\top \mathbf{x} & \textbf{(Linear Relaxation)} & \\
\text{s.t. } \mathbf{Ax} \leq \mathbf{b} & \max_{\mathbf{y}} [\mathbf{b}^\top, \mathbf{1}^\top] \mathbf{y} & \mathbf{Ax} + \mathbf{r} = \mathbf{b} \\
\mathbf{x} \leq 1 & \text{s.t. } [\mathbf{A}^\top, \mathbf{I}] \mathbf{y} \geq \mathbf{c} & [\mathbf{A}^\top, \mathbf{I}] \mathbf{y} - \mathbf{s} = \mathbf{c} \\
\mathbf{x} \geq 0 & & \mathbf{r} \geq 0 \\
\mathbf{x} \in \mathbb{Z} & & \mathbf{s} \geq 0
\end{array} \tag{14} \tag{15} \tag{16}$$

Considering the inherent structure of binary MILP, we can further decompose the dual solution \mathbf{y} into two parts: \mathbf{y}_1 (corresponding to regular constraints $\mathbf{Ax} \leq \mathbf{b}$) and \mathbf{y}_2 (corresponding to constraints $\mathbf{x} \leq 1$). The encoding of binary MILP problem into a bipartite VC graph is illustrated in Table. 8. And the decoder could be models as Equation. 17.

$$\begin{aligned}
p_\theta(G|G', \mathbf{z}) &= p_\theta(d_{c_i} | \mathbf{h}_{c_i}^{G'}, \mathbf{z}_{c_i}) \cdot \prod_{u \in \mathcal{V}} p_\theta(e(c_i, u) | \mathbf{h}_V^{G'}, \mathbf{z}_V) \cdot \prod_{u \in \mathcal{V}: e(c_i, u)=1} p_\theta(w_{c_i} | \mathbf{h}_V^{G'}, \mathbf{z}_V) \\
&\cdot \prod_{u \in \mathcal{C}} p_\theta(\mathbf{y}_{1u} | \mathbf{h}_C^{G'}, \mathbf{z}_C) p_\theta(\mathbf{r}_u | \mathbf{h}_C^{G'}, \mathbf{z}_C) \cdot \prod_{u \in \mathcal{V}} p_\theta(\mathbf{x}_u | \mathbf{h}_V^{G'}, \mathbf{z}_V) p_\theta(\mathbf{s}_u | \mathbf{h}_V^{G'}, \mathbf{z}_V) p_\theta(\mathbf{y}_{2u} | \mathbf{h}_V^{G'}, \mathbf{z}_V),
\end{aligned} \tag{17}$$

where the decoder of DIG-MILP specifically designed for binary MILP partitions the predicted dual solution \mathbf{y} into two segments $\mathbf{y}_1, \mathbf{y}_2$ and predict each segment separately.

Table 8: V-C encoding for binary MILP.

object	feature
constraint	all 0's
node	$\mathbf{y}_1 = \{\mathbf{y}_{11} \dots \mathbf{y}_{1m}\}$
$\mathcal{C} = \{c_1 \dots c_m\}$	$\mathbf{r} = \{\mathbf{s}_1 \dots \mathbf{s}_m\}$
variable	all 1's
node	$\mathbf{x} = \{\mathbf{x}_1 \dots \mathbf{x}_n\}$
$\mathcal{V} = \{v_1 \dots v_n\}$	$\mathbf{s} = \{\mathbf{r}_1 \dots \mathbf{r}_n\}$
edge \mathcal{E}	$\mathbf{y}_2 = \{\mathbf{y}_{21} \dots \mathbf{y}_{2n}\}$
	non-zero weights in \mathbf{A}

Hyper-parameters Across the four datasets, we set the same learning rate for DIG-MILP as $1e - 3$. We use the Adam optimizer (Kingma & Ba, 2014). For the SC, we set the α in $\mathcal{L}_{\theta, \phi}$ as 5, for the CA, the CVS, and the IIS, we set α as 150. We use the random seed as 123 for DIG-MILP training across all the four datasets.

B.3 Implementation of baseline

‘Bowly’ Here we show the implementation of generating instances from scratch with the baseline Bowly (Bowly, 2019). The generation of matrix \mathbf{A} is illustrated in the algorithm. 3. With the generated adjacency matrix \mathbf{A} , where we manipulate the hyper-parameters during the generation process to ensure that the statistical properties of \mathbf{A} align as closely as possible with the original dataset. Specifically, we keep the size of graph (m, n) the same as the original dataset and uniformly sample p_v, p_c from $[0, 1]$ for all the four datasets. For the other hyper-parameter settings, see Tables. 9.

Then we uniformly sample the solution space $\mathbf{x}, \mathbf{y}, \mathbf{s}, \mathbf{r}$ with intervals defined by their corresponding maximum and minimum from the training dataset. Then we deduce \mathbf{b}, \mathbf{c} to get the new MILP instances.

‘Random’ We use exactly the same network architecture and generation process as DIG-MILP. The key difference is that instead of utilizing the trained NN, we uniformly sample the variables $d_{c_i}, e(c_i, u), w_{c_i}, \mathbf{y}_1, \mathbf{s}, \mathbf{x}, \mathbf{r}, \mathbf{y}_2$ required for decoder prediction within intervals delineated by the maximum

Algorithm 3 Bowly - generation of matrix **A****Require:** $n \in [1, \infty), m \in [1, \infty), \rho \in (0, 1], p_v \in [0, 1], p_c \in [0, 1], \mu_A \in (-\infty, \infty), \sigma_A \in (0, \infty)$ **Ensure:** Constraint matrix $\mathbf{A} \in \mathbb{Q}^{m \times n}$

```

1: Set target variable degree  $d(u_i) = 1$  for randomly selected  $i, 0$  for all others
2: Set target constraint degree  $d(v_j) = 1$  for randomly selected  $j, 0$  for all others
3:  $e \leftarrow 1$ 
4: while  $e < pmn$  do
5:    $s \leftarrow$  draw  $n$  values from  $U(0, 1)$ 
6:    $t \leftarrow$  draw  $m$  values from  $U(0, 1)$ 
7:   Increment the degree of variable node  $i$  with maximum  $p_v \frac{d(u_i)}{e} + s_i$ 
8:   Increment the degree of constraint node  $j$  with maximum  $p_c \frac{d(v_j)}{e} + t_j$ 
9:    $e \leftarrow e + 1$ 
10: end while
11: for  $i = 1, \dots, n$  do
12:   for  $j = 1, \dots, m$  do
13:      $r \leftarrow$  draw from  $U(0, 1)$ 
14:     if  $r < \frac{d(u_i)d(v_j)}{e}$  then
15:       Add edge  $(i, j)$  to VC
16:     end if
17:   end for
18: end for
19: while  $\min((d(u_i), d(v_j)) = 0$  do
20:   Choose  $i$  from  $\{i | d(u_i) = 0\}$ , or randomly if all  $d(u_i) > 0$ 
21:   Choose  $j$  from  $\{j | d(v_j) = 0\}$ , or randomly if all  $d(v_j) > 0$ 
22:   Add edge  $(i, j)$  to VC
23: end while
24: for  $(i, j) \in E(VC)$  do
25:    $a_{ij} = \mathcal{N}(\mu_A, \sigma_A)$ 
26: end for
27: return A

```

Table 9: The hyper-parameter selection of the Bowly baseline.

	density	$\mu_{\mathbf{A}}$	$\sigma_{\mathbf{A}}$
SC	$\mathcal{U}\{0.15, 0.20, 0.25, 0.30, 0.35\}$	-1	0
CA	0.05	1	$\mathcal{U}(0.1, 0.3)$
CVS	0.0013	0.2739	0.961
IIS	0.0488	-1	0

and minimum values of each variable from the training set, simulating the random parameters of an untrained neural network.

B.4 Implementation of the structural statistical characteristics

The explanation of various statistical metrics used for comparing the structural similarity of MILP problem instances is detailed as shown in Table. 10. Specific numerical values for different metrics for the SC and CA problems can be found in Table. 13 and Table. 14, respectively.

Table 10: Explanation of the statistic metrics of the MILP instances

name	explanation
density mean	the average number of non zero values in the constraint matrix
cons degree mean	the average number of constraint node degree
cons degree std	the standard variance of constraint node degree
var degree mean	the average number of variable node degree
var degree std	the standard variance of variable node degree
\mathbf{b} mean	the average \mathbf{b} value
\mathbf{b} std	the standard variance of \mathbf{b} value
\mathbf{c} mean	the average value of \mathbf{c}
\mathbf{c} std	the standard variance of \mathbf{c} value

For each statistic metric i shown in Table. 10, we begin by collecting lists of the values from four data sources: the original dataset, the data generated by the ‘Bowly’ baseline, the data generated by the ‘random’ baseline, and data generated by DIG-MILP. Each data source contains 1000 instances. We then employ the lists from the four data sources to approximate four categorical distributions. Utilizing the *numpy.histogram* function, we set the number of bins to the default value of 10, with the min and max values derived from the collective minimum and maximum of a given metric across the four data sources, respectively. Next, we employ Jensen-Shannon (JS) divergence D_{js}^i via the function *scipy.spatial.distance.jensenshannon* (Virtanen et al., 2020) to quantify the divergence between the original samples and the rest three data sources, resulting in score_i for each statistical metric.

$$\text{score}_i = (\max(D_{js}) - D_{js}^i) / (\max(D_{js}) - \min(D_{js})), \quad (18)$$

where $\max(D_{js}), \min(D_{js})$ are the maximum and minimum of JS divergence across all the metrics.

Then we average the score for each statistic metric to obtain the final similarity score, as is shown in Table. 12:

$$\text{score} = \frac{1}{9} \sum_{i=1}^9 \text{score}_i. \quad (19)$$

B.5 Implementation of Data Sharing for Solver Configuration Tuning

Below are the hyper-parameters that we randomly sample to test the positive-correlation of different dataset pairs. We adhere to the configuration established in mainstream solver tuning literature to select the pa-

parameters requiring adjustment Hutter et al. (2011); Lindauer & Hutter (2018); Lindauer et al. (2022), . For a detailed explanation of each parameter, please refer to the SCIP documentation⁶.

Table 11: The selected SCIP hyper-parameters and the range to randomly select from.

params	whole range/choice	default	our range/choice
branching/scorefunc	s, p, q	s	s, p, q
branching/scorefac	[0, 1]	0.167	[0, 1]
branching/preferbinary	True, False	False	True, False
branching/clamp	[0,0.5]	0.2	[0,0.5]
branching/midpull	[0,1]	0.75	[0,1]
branching/midpullreldomtrig	[0,1]	0.5	[0,1]
branching/lpgainnormalize	d, l, s	s	d, l, s
lp/pricing	l, a, f, p, s, q, d	l	l, a, f, p, s, q, d
lp/colagelimit	[-1,2147483647]	10	[0,100]
lp/rowagelimit	[-1,2147483647]	10	[0,100]
nodeselection/childsel	d, u, p, I, l, r, h	h	d, u, p, I, l, r, h
separating/minortho	[0,1]	0.9	[0,1]
separating/minorthoroot	[0,1]	0.9	[0,1]
separating/maxcuts	[0,2147483647]	100	[0,1000]
separating/maxcutsroot	[0,2147483647]	2000	[0,10000]
separating/cutagelimit	[-1,2147483647]	80	[0,200]
separating/poolfreq	[-1,65534]	10	[0,100]

B.6 Implementation of Optimal Value Prediction via ML

Neural Network Architecture In this downstream task, We also use the bipartite GNN backbone which is exactly the same as that in Gasse et al. (2019). We use an MLP layer and global mean pooling to produce the optimal objective value prediction. The learning rate is set as $1e - 3$.

C Supplementary Experiment Results

C.1 statistical characteristics of the generated instances

Table 12: The similarity score \uparrow between the original and generated data .

constraint	replace rates γ	-	0.01	0.05	0.10	0.20	0.50
SC	Bowly	0.337	-	-	-	-	-
	random	-	0.701	0.604	0.498	0.380	0.337
	ours	-	0.856	0.839	0.773	0.652	0.570
CA	Bowly	0.386	-	-	-	-	-
	random	-	0.630	0.566	0.508	0.432	0.306
	ours	-	0.775	0.775	0.768	0.733	0.630

We compare the statistical metrics between the generated instances and the original instances on the SC and CA datasets. We do not calculate the statistics on the CVS and IIS due to their limited size that prevents meaningful statistical comparisons. We count nine statistic metrics in total, see Table. B.4 in the appendix for details. The similarity score is derived from the Jensen-Shannon (JS) divergence (the lower the better) between each metric of the generated and original data, as shown in Table. 12. ‘Bowly’ shows the least similarity. As the the constraint replacement ratio γ increases from 0.01 to 0.50, the table shows a decreasing similarity between new and original instances for both DIG-MILP and ‘random’, aligning with our expectation of controlling structural similarity by adjusting the number of constraint nodes to replace. Instances generated by DIG-MILP more closely mirror the target data in structural statistical metrics across all γ . For detailed calculations of the similarity score and the specific values of each statistic

⁶<https://www.scipopt.org/doc/html/PARAMETERS.php>

Table 13: Statistic value comparison across the original dataset and the generated datasets with different constraints replacement rates on the set covering (SC) problem. ‘resolving time’ calculates under default configuration of pySCIPopt. ‘density’ represents the ratio of non zero entries in the constraint matrix. ‘cons degree’ denotes the degree of constraint nodes, ‘var degree’ stands for the degree of variable nodes. \mathbf{b} denotes the right hand side vector of the MILP, and \mathbf{c} is the objective coefficient vector.

	replace ratio	resolving time (s)	density mean	cons degree mean	cons degree std	var degree mean	var degree std	b mean	b std	c mean	c std
original	-	0.821	0.251	100.700	8.447	50.350	6.854	-1.0	0.0	50.490	28.814
Bowly	-		0.205	82.312	35.131	41.305	21.628	1.484	3.504	403.208	198.571
random	0.01	127.723	0.251	100.774	9.853	50.387	6.841	1.294	3.045	422.65	65.078
random	0.05	143.883	0.253	101.039	14.070	50.519	6.787	1.218	3.123	431.422	66.082
random	0.10	187.851	0.253	101.357	17.706	50.678	6.727	1.164	3.210	441.696	67.250
random	0.20	304.216	0.255	101.900	22.808	50.950	6.607	1.062	3.351	460.696	69.379
random	0.50	1312.595	0.258	103.348	31.305	51.674	6.375	0.664	3.629	509.337	74.864
ours	0.01	83.681	0.251	100.700	8.876	50.350	7.431	-0.515	1.351	44.863	0.939
ours	0.05	70.476	0.251	100.712	10.202	50.356	9.977	-0.456	1.386	44.958	0.984
ours	0.10	54.650	0.251	100.738	11.365	50.369	13.354	-0.413	1.441	45.057	1.032
ours	0.20	54.830	0.251	100.754	12.872	50.377	19.992	-0.368	1.576	45.112	1.071
ours	0.50	22.462	0.252	100.830	14.433	50.415	37.017	-0.005	1.271	44.967	1.872

Table 14: Statistic value comparison across the original dataset and the generated datasets with different constraints replacement rates on the combinatorial auction (CA) problem. ‘resolving time’ calculates under default configuration of pySCIPopt. ‘density’ represents the ratio of non zero entries in the constraint matrix. ‘cons degree’ denotes the degree of constraint nodes, ‘var degree’ stands for the degree of variable nodes. \mathbf{b} denotes the right hand side vector of the MILP, and \mathbf{c} is the objective coefficient vector.

	replace ratio	resolving time (s)	density mean	cons degree mean	cons degree std	var degree mean	var degree std	b mean	b std	c mean	c std
original	-	1.360	0.050	14.538	13.834	5.578	3.253	1.0	0.0	330.999	234.444
Bowly	-	0.281	0.048	14.415	13.633	5.544	7.262	1.668	1.617	510.211	1101.065
random	0.01	0.416	0.051	14.664	13.970	5.634	3.240	1.748	1.602	524.961	563.436
random	0.05	0.502	0.054	15.225	14.531	5.878	3.201	1.792	1.647	560.369	561.074
random	0.10	0.555	0.056	15.877	15.088	6.152	3.161	1.855	1.706	598.047	555.956
random	0.20	0.821	0.061	17.098	15.953	6.658	3.106	1.966	1.797	669.168	552.853
random	0.30	1.056	0.065	18.186	16.527	7.105	3.070	2.053	1.850	735.284	548.606
random	0.50	2.353	0.072	19.959	17.222	7.837	3.006	2.267	1.972	841.971	545.471
ours	0.01	0.361	0.050	14.490	13.776	5.565	3.253	1.645	1.348	361.711	264.798
ours	0.05	0.360	0.050	14.361	13.609	5.535	3.286	1.609	1.325	351.417	261.927
ours	0.10	0.301	0.050	14.205	13.401	5.500	3.366	1.589	1.329	342.702	261.313
ours	0.20	0.217	0.049	13.819	12.854	5.412	3.586	1.525	1.315	324.282	260.848
ours	0.30	0.140	0.047	13.454	12.330	5.344	3.847	1.454	1.280	304.911	260.949
ours	0.50	0.055	0.045	12.869	11.379	5.254	4.282	1.350	1.233	271.474	255.515

metric, see B.4 and C.1 in the appendix. The detailed dynamic ranges of CA and SC could be found in https://miplib.zib.de/tag_collection.html.

C.2 Data Sharing for Solver configuration Tuning

CVS and IIS There are five total instances in CVS, comprising three for training DIG-MILP and the downstream predictor and two for testing. The IIS has two instances, one for training and one for testing (with allocation based on alphabetical order). Please refer to Table. 15 for the model’s performance. ‘ground truth’ corresponds to the true values of the optimal objectives for each problem. Models trained exclusively on the ‘original’ training set exhibit superior fitting and more accurate predictions on the training set itself. However, models trained on the datasets where we introduce 20 additional newly generated instances by DIG-MILP with varying constraint replacement ratio γ not only demonstrate minimal gap in prediction on the training set towards the models trained solely on the original data compared with the baselines, but also showcase improved predictive performance on previously unseen test sets. This underscores the notion that the DIG-MILP-generated data can indeed increase structural and solution label diversity to a certain extent, thereby enhancing the generalization capability and overall performance of the models. Again, similar to the previous two experiments, ‘Bowly’ degrades the predictive performance of the model, ‘random’ results in marginal improvement in out-of-distribution prediction accuracy.

Table 15: The predicted value and relative mean square error (MSE) of the optimal objective value on the CVS and the IIS problem. In the CVS, ‘cvs08r139-94’, ‘cvs16r70-62’, ‘cvs16r89-60’ are used as training data, ‘cvs16r106-72’, ‘cvs16r128-89’ are used as testing data. In the IIS, ‘iis-glass-cov’ is used as the training data, ‘iis-hc-cov’ is used as the testing data. ‘original’ shows the performance of the model trained merely on the three (CVS) or single (IIS) original training instances.

		in-distribution						out-of-distribution				in-distribution		out-of-distribution	
		cvs08r139-94		cvs16r70-62		cvs16r89-60		cvs16r106-72		cvs16r128-89		iis-glass-cov		iis-hc-cov	
dataset	ratio	value	msre	value	msre	value	msre	value	msre	value	msre	value	msre	value	msre
ground truth	-	116	0	42	0	65	0	81	0	97	0	-17	0	-21	0
original	-	115.994	2e-9	41.998	1e-9	64.997	1e-9	77.494	0.001	89.258	0.006	-20.999	3e-10	-94.451	20.756
Bowly	-	65.712	0.187	82.353	0.923	66.858	8e-6	61.504	0.057	66.045	0.101	-88.756	17.816	-88.756	17.816
random	0.01	138.459	0.037	45.312	0.006	67.875	0.001	58.754	0.075	68.192	0.088	-22.263	3e-4	-83.146	15.139
random	0.05	163.412	0.167	34.571	0.031	45.605	0.089	41.110	0.242	24.952	0.551	-20.695	2e-4	-82.297	14.753
random	0.10	116.824	5e-5	60.440	0.192	79.152	0.047	68.641	0.023	79.321	0.033	-20.991	1e-7	-807.680	2163.238
random	0.20	144.962	0.062	79.849	0.812	99.552	0.282	71.821	0.0128	99.898	8e-4	-21.678	0.001	-227.610	153.482
random	0.50	159.807	0.142	49.364	0.030	65.213	1e-5	103.960	0.080	122.321	0.068	-21.633	9e-3	-100.224	23.966
DIG-MILP	0.01	116.981	7e-5	42.197	2e-5	64.876	3e-6	78.646	8e-4	96.831	3e-6	-20.933	1e-5	-90.556	18.721
DIG-MILP	0.05	161.558	0.154	26.181	0.141	23.439	0.408	66.119	0.033	76.119	0.046	-21.108	2e-5	-61.217	6.765
DIG-MILP	0.10	118.609	5e-4	45.461	0.006	67.216	0.001	80.706	1e-5	95.745	1e-4	-20.976	1e-6	-65.385	8.101
DIG-MILP	0.20	114.622	1e-4	42.933	4e-4	62.627	0.001	83.379	8e-4	120.641	0.0594	-20.159	0.001	-55.926	5.243
DIG-MILP	0.50	120.361	0.001	44.472	0.003	69.287	0.004	84.870	0.002	104.333	0.005	-21.009	2e-7	-90.427	18.655

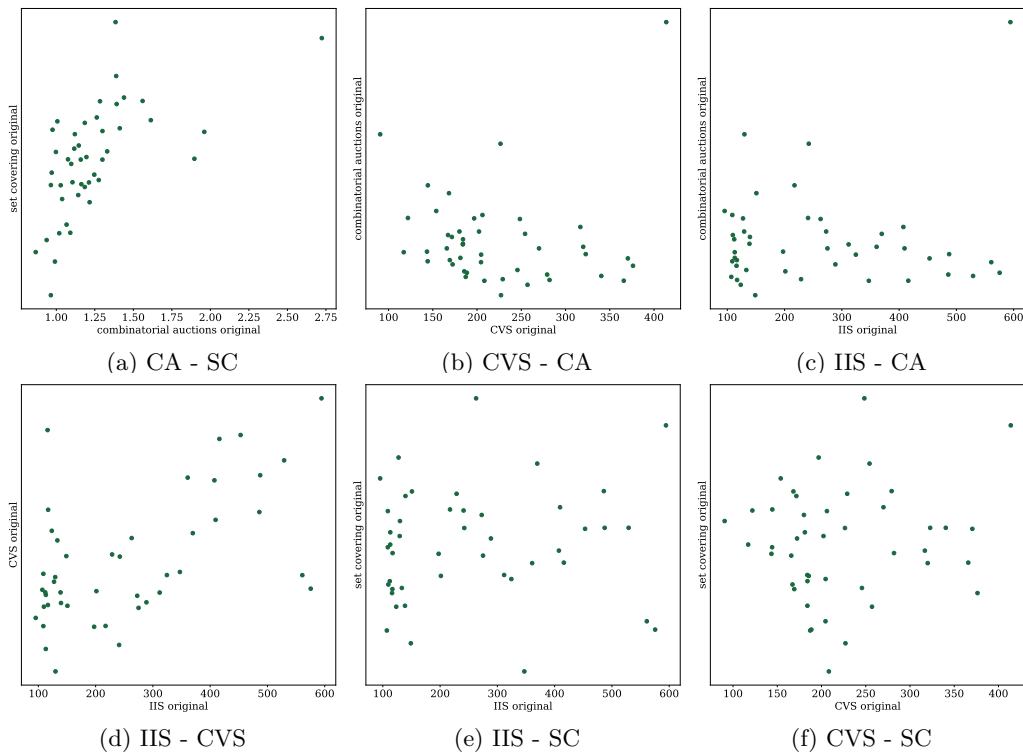


Figure 5: The solution time of SCIP with different parameter sets across different original datasets.

We present the visual results for CA, SC, and IIS datasets, see Fig. 6, 7, 8.

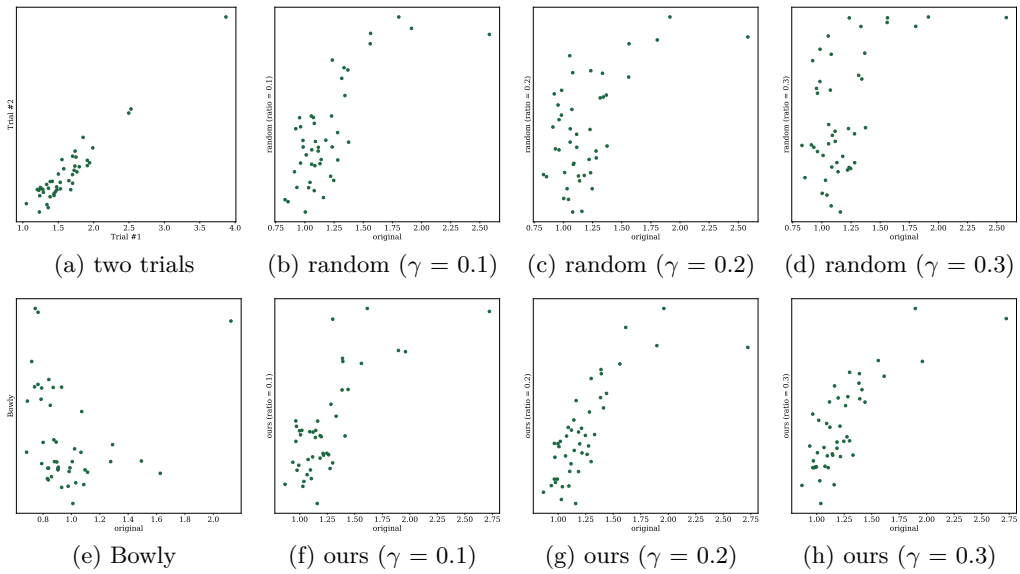


Figure 6: The solution time of SCIP on the CA with 45 different hyper-parameter sets.

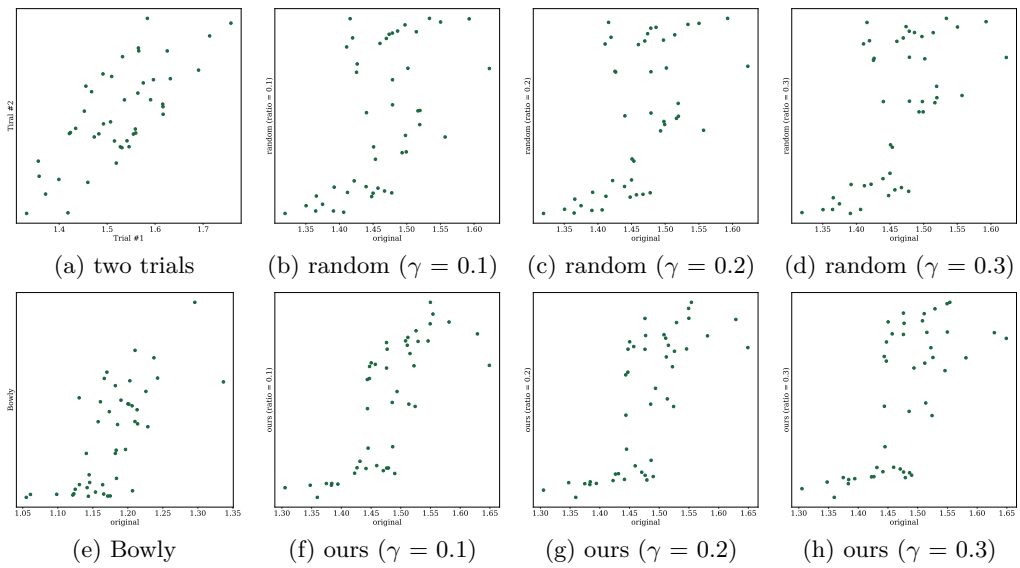


Figure 7: The solution time of SCIP on the SC with 45 different hyper-parameter sets.

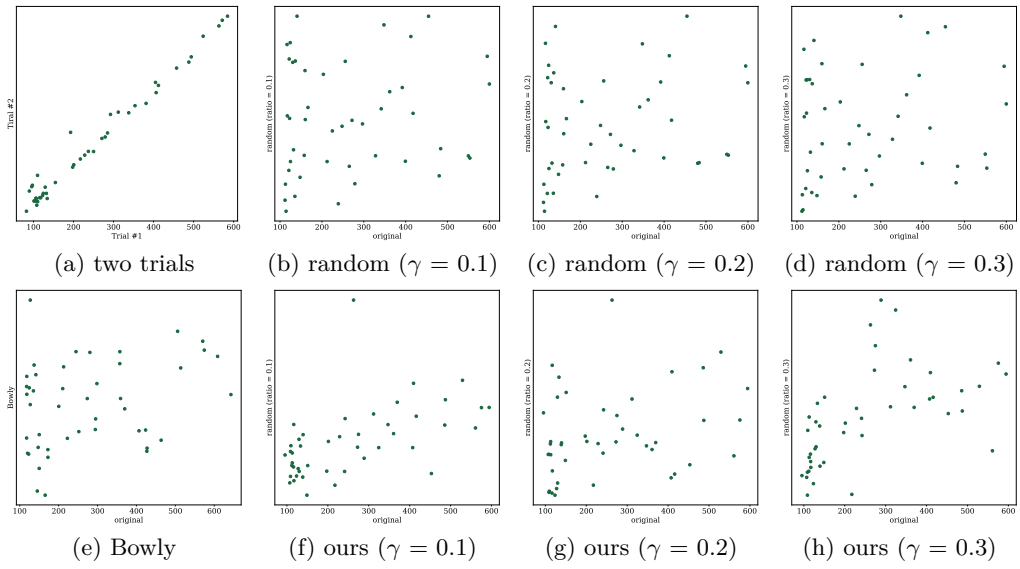


Figure 8: The solution time of SCIP on the IIS with 45 different hyper-parameter sets.